

# Loop correction and resummation of vertex functions for a self interacting scalar field in the de Sitter spacetime

<sup>1</sup>Sourav Bhattacharya\* and <sup>2</sup>Sudesh Kumar<sup>†</sup>

<sup>1</sup>Relativity and Cosmology Research Centre, Department of Physics, Jadavpur University, Kolkata 700 032, India

<sup>2</sup>Department of Physics, Indian Institute of Technology Ropar, Rupnagar, Punjab 140 001, India

December 7, 2023

## Abstract

We consider a massless and minimally coupled self interacting quantum scalar field theory in the inflationary de Sitter background of dimension four. The self interaction potential is taken to be either quartic,  $\lambda\phi^4/4!$ , or quartic plus cubic,  $\lambda\phi^4/4! + \beta\phi^3/3!$  ( $\lambda > 0$ ). We compute the four and three point vertex functions up to two loop. The purely local or partly local part of these renormalised loop corrected vertex functions grow unboundedly after sufficient number of de Sitter  $e$ -foldings, due to the appearances of secular logarithms. We focus on the purely local part of the vertex functions and attempt a resummation of them in terms of the dynamically generated mass of the scalar field at late times. It turns out that the resummed, non-perturbative effective vertex functions have values less than that of the tree level. The variation of these vertex functions are investigated with respect to the tree level couplings numerically. Since neither the secular effect, nor the dynamical generation of field mass is possible in the Minkowski spacetime, the above phenomenon has no flat spacetime analogue.

**Keywords :** Massless minimal scalar field, de Sitter spacetime, secular effect, vertex functions, loop correction, resummation

---

\*sbhatta.physics@jadavpuruniversity.in

<sup>†</sup>sudesh.21phz0007@iitrpr.ac.in

# Contents

<b>1</b>	<b>Introduction</b>	<b>2</b>
<b>2</b>	<b>A brief review of the basic ingredients</b>	<b>3</b>
<b>3</b>	<b>Loop correction to the four point vertex</b>	<b>5</b>
3.1	One loop . . . . .	5
3.2	Two loop . . . . .	7
<b>4</b>	<b>Loop correction to the cubic vertex function</b>	<b>11</b>
4.1	One loop . . . . .	12
4.2	Two loop . . . . .	12
<b>5</b>	<b>Non-perturbative values of the vertex functions via the dynamical mass generation</b>	<b>14</b>
<b>6</b>	<b>Discussion</b>	<b>18</b>
<b>A</b>	<b>The diagrams with purely non-local contributions but no non-vanishing flat spacetime limit</b>	<b>19</b>

## 1 Introduction

The standard cosmological model predicts that our universe started expanding with a big bang, while the rate of expansion always decreasing monotonically. As such, this model has been very successful in predicting the redshift of galaxies, the cosmic microwave background radiation, the abundances of light elements and so on. However, several other important issues like the observed spatial flatness of our universe at present, the observed high degree of isotropy at very large scales and the rarity/unobservability of relics like the magnetic monopoles cannot be explained by this standard big bang model. The primordial cosmic inflation is a proposed phase of very rapid, near exponential accelerated expansion of our very early universe, in order to provide a possible solution to these problems. Indeed, the inflationary phase not only offers satisfactory answers to these aforementioned puzzles, but also provides a robust mechanism to generate primordial cosmological density perturbations, as the seed to the cosmic web we observe in the sky today at large scales. We refer our reader to [1, 2] and references therein for excellent pedagogical discussion on these issues.

In general relativity, the accelerated expansion of the spacetime always necessitates some exotic matter field with positive energy density but negative, isotropic pressure, known as the dark energy. The simplest form the dark energy is just the cosmological constant,  $\Lambda$ . A slowly rolling scalar field off a potential can also work effectively as dark energy. However, such description lacks any microscopic quantum description, which can be large in a time dependent background. Now, the current observed density of dark energy is naturally much small compared to that of the primordial inflationary one. It turns out that only about 10% mismatch of the current dark energy density would have led to drastic changes in the formation of large scale structures. Thus it is an interesting question to ask, how did  $\Lambda$ /dark energy attained today's tiny value? This is known as the cosmic coincidence puzzle [3, 4, 5] (also references therein). We also refer our reader to e.g. [6, 7, 8, 9, 10, 11] for alternative proposals to the solution to this problem. In particular, could the backreaction of the inflationary quantum fields screen the inflationary  $\Lambda$ ? We shall be chiefly concerned about this question in this paper.

In particular, a massless quantum field theory with zero rest mass but not conformally invariant (e.g., gravitons and massless minimally coupled scalars) can generate de Sitter breaking large loop corrections growing monotonically with time, proportional to the logarithm of the scale factor, known as the *secular effect*. This indicates that after sufficient

number of  $e$ -foldings the perturbation theory breaks down, necessitating some resummation [12]. This is essentially an infrared effect originating from the accumulation of the long wavelength modes after crossing the Hubble horizon. For a massless minimally coupled scalar, such infrared contributions can be resummed, to produce for example, a finite two point correlation function. The issue of performing such resummation for gravitons however, remains as an open question, e.g. [5] (also references therein).

Free quantum field quantisation in the de Sitter spacetime can be seen in [13, 14, 15, 16, 17, 18, 19]. It is well known by now that a massless and minimally coupled scalar field cannot have a de Sitter invariant vacuum state or two point function. For such a scalar with self interaction, the loops then naturally show de Sitter breaking effect growing monotonically with time mentioned above, e.g. [20, 21, 22, 23, 24, 25, 26, 27, 28, 29, 30, 31, 32, 33, 34] and references therein. Efforts to resum such non-perturbative infrared effect (appears as the logarithm of the scale factor) by various methods can be seen in e.g. [5, 35, 36, 37, 38, 39, 40, 41, 42, 43, 44, 45, 46, 47, 48, 49, 50, 51, 52, 53, 54]. We also refer our reader to [55, 56] (see also [57, 58, 59, 60, 61, 62, 63, 64, 65] for recent developments) for a stochastic formulation for resumming correlation functions at late times for self interacting scalar field theory in the inflationary background. Perhaps one of the most important prediction of this resummation is the emergence of a dynamically generated scalar mass at late times [56, 66, 67]. This is certainly a manifestation of strong quantum fluctuations. The dynamical mass may leave interesting footprints into the cosmic microwave background.

How does the secular effect affect the vertex functions in a self interacting quantum field theory in a non-perturbative manner? To the best of our knowledge, this question has not so far been addressed systematically in the literature. Precisely, we wish to compute in this paper the quartic and cubic vertex functions up to two loop for quartic and quartic plus cubic self interactions, respectively  $V(\phi) = \lambda\phi^4/4!$  and  $V(\phi) = \lambda\phi^4/4! + \beta\phi^3/3!$  ( $\lambda > 0$ ). For a quartic self interaction, the one loop correction to the four point vertex can be seen in [21]. These results show, as expected, secularly growing logarithms. We further wish to resum these expressions in terms of the late time dynamically generated scalar mass. The rest of the paper is organised as follows. After briefly reviewing the necessary ingredients in the next section, we compute the renormalised one and two loop corrections to the quartic and cubic vertex functions respectively in Section 3 and Section 4 and Appendix A. The resulting secular logarithms for the purely local part of the vertex functions are then resummed in terms of the dynamically generated scalar mass in Section 5, to yield a finite answer at late times. We argue this resummation can essentially be represented via daisy-like Feynman graphs. It turns out that the resummed, non-perturbative effective vertex functions have values less than that of the tree level. Finally, we conclude in Section 6.

We shall work with the mostly positive signature of the metric in  $d = 4 - \epsilon$  ( $\epsilon = 0^+$ ) dimensions and will set  $c = 1 = \hbar$  throughout. Also for the sake of brevity, we shall denote for powers of propagators and logarithms respectively as,  $(i\Delta)^n \equiv i\Delta^n$  and  $(\ln x)^n \equiv \ln^n x$ .

## 2 A brief review of the basic ingredients

We begin with the metric of the cosmological de Sitter spacetime

$$ds^2 = -dt^2 + a^2(t)d\vec{x} \cdot d\vec{x} = a^2(\eta) (-d\eta^2 + d\vec{x} \cdot d\vec{x}) \quad (1)$$

where the scale factor  $a(t)$  equals  $e^{Ht}$  with  $H^2 = \Lambda/3$ ,  $\Lambda$  being the positive cosmological constant.  $t$  and  $\eta$  are respectively called the cosmological and conformal time, with  $\eta = -e^{-Ht}/H$ , thus  $a(\eta) = -1/H\eta$ . The de Sitter metric has a symmetry of time translation followed by a coordinate scaling. Utilising this symmetry, we set the temporal range  $0 \leq t < \infty$ , so that  $-H^{-1} \leq \eta < 0^-$ .

We take the bare Lagrangian density to be that of a scalar field  $\psi'$ , with quartic and cubic self interaction potential

$$S = \int \sqrt{-g} d^d x \left[ -\frac{1}{2} g^{\mu\nu} (\nabla_\mu \psi') (\nabla_\nu \psi') - \frac{1}{2} m_0^2 \psi'^2 - \frac{\lambda_0}{4!} \psi'^4 - \frac{\beta_0}{3!} \psi'^3 - \tau_0 \psi' \right] \quad (2)$$

We define the field strength renormalisation,  $\phi = \psi' / \sqrt{Z}$ , so that

$$S = \int d^d x \left[ -\frac{Z}{2} \eta^{\mu\nu} a^{d-2} (\partial_\mu \phi) (\partial_\nu \phi) - \frac{1}{2} Z m_0^2 \phi^2 a^d - \frac{Z^2 \lambda_0}{4!} \phi^4 a^d - \frac{\beta_0 Z^{3/2}}{3!} \phi^3 a^d - \tau_0 \sqrt{Z} \phi a^d \right] \quad (3)$$

We take the rest mass of the field to be vanishing, so that

$$Z = 1 + \delta Z \quad Z m_0^2 = 0 + \delta m^2 \quad Z^2 \lambda_0 = \lambda + \delta \lambda \quad \beta_0 Z^{3/2} = \beta + \delta \beta \quad \tau_0 \sqrt{Z} = \alpha \quad (4)$$

where  $\delta m^2$ ,  $\delta \lambda$ ,  $\delta \beta$  and  $\alpha$  are counterterms. Substituting now the above into Eq. (3), we have

$$S = \int d^d x \left[ -\frac{1}{2} \eta^{\mu\nu} a^{d-2} (\partial_\mu \phi) (\partial_\nu \phi) - \frac{\lambda}{4!} \phi^4 a^d - \frac{\beta}{3!} \phi^3 a^d - \frac{\delta Z}{2} \eta^{\mu\nu} a^{d-2} (\partial_\mu \phi) (\partial_\nu \phi) - \frac{1}{2} \delta m^2 \phi^2 a^d - \frac{\delta \lambda}{4!} \phi^4 a^d - \frac{\delta \beta}{3!} \phi^3 a^d - \alpha \phi a^d \right] \quad (5)$$

Note that the above quartic plus cubic potential (with  $\lambda > 0$ ) is the most general renormalisable self interaction in four spacetime dimensions.

The mode functions for a free massless scalar field ( $\square \phi = 0$ ) reads

$$\phi_k(x) = \frac{H}{\sqrt{2k^3}} (1 + ik\eta) e^{-ik\eta + i\vec{k} \cdot \vec{x}} \quad (k \equiv |\vec{k}|)$$

along with its complex conjugation. With these mode functions, the one can make the canonical quantisation on some initial hypersurface. We take this initial surface to be at  $\eta = -1/H$  and also for the initial sub-Hubble modes,  $k/H \gg 1$ . The corresponding mode functions are known as the Bunch-Davies vacuum [13, 14]. However, it is easy to check that these mode functions do not remain normalised afterwards. Accordingly, there is not de Sitter invariant two point function in the de Sitter spacetime [17, 18].

The propagator for a massless and minimally coupled scalar field with respect to the initial Bunch-Davies vacuum state reads, e.g. [21],

$$i\Delta(x, x') = A(x, x') + B(x, x') + C(x, x') \quad (6)$$

where

$$\begin{aligned} A(x, x') &= \frac{H^{2-\epsilon} \Gamma(1-\epsilon/2)}{4\pi^{2-\epsilon/2}} \frac{1}{y^{1-\epsilon/2}} \\ B(x, x') &= \frac{H^{2-\epsilon}}{(4\pi)^{2-\epsilon/2}} \left[ -\frac{2\Gamma(3-\epsilon)}{\epsilon} \left(\frac{y}{4}\right)^{\epsilon/2} + \frac{2\Gamma(3-\epsilon)}{\epsilon\Gamma(2-\epsilon/2)} + \frac{2\Gamma(3-\epsilon)}{\Gamma(2-\epsilon/2)} \ln(aa') \right] \\ C(x, x') &= \frac{H^{2-\epsilon}}{(4\pi)^{2-\epsilon/2}} \sum_{n=1}^{\infty} \left[ \frac{\Gamma(3-\epsilon+n)}{n\Gamma(2-\epsilon/2+n)} \left(\frac{y}{4}\right)^n - \frac{\Gamma(3-\epsilon/2+n)}{(n+\epsilon/2)\Gamma(2+n)} \left(\frac{y}{4}\right)^{n+\epsilon/2} \right] \end{aligned} \quad (7)$$

where the de Sitter invariant interval is given by

$$y(x, x') = aa' H^2 \Delta x^2 = aa' H^2 \left[ |\vec{x} - \vec{x}'|^2 - (\eta - \eta')^2 \right] \quad (8)$$

Note that  $y(x, x')$  is proportional to the invariant interval of the Minkowski spacetime,  $\Delta x^2$ , owing to the former's conformal flatness.

In general in a non-equilibrium background such as the de Sitter, often the in-in or the Schwinger-Keldysh formalism needs to be used, e.g. [68, 69, 42, 70]. There are total four propagators in this formalism, characterised by suitable four complexified distance functions

$$\begin{aligned}\Delta x_{++}^2 &= \left[ |\vec{x} - \vec{x}'|^2 - (|\eta - \eta'| - i\epsilon)^2 \right] = (\Delta x_{--}^2)^* \\ \Delta x_{+-}^2 &= \left[ |\vec{x} - \vec{x}'|^2 - ((\eta - \eta') + i\epsilon)^2 \right] = (\Delta x_{-+}^2)^* \quad (\epsilon = 0^+)\end{aligned}\quad (9)$$

The first two correspond respectively to the Feynman and anti-Feynman propagators, whereas the last two correspond to the two Wightman functions. However for our present purpose, as we shall see, we require the Feynman propagator only. The tree level propagators satisfy

$$\square_x i\Delta_{ss'}(x, x') = i s \delta_{ss'} \delta^d(x - x') \quad s, s' = \pm$$

We have in the coincidence limit for all the four propagators

$$i\Delta(x, x) = \frac{H^{2-\epsilon}\Gamma(2-\epsilon)}{2^{2-\epsilon}\pi^{2-\epsilon/2}\Gamma(1-\epsilon/2)} \left( \frac{1}{\epsilon} + \ln a \right) \quad (10)$$

$i\Delta(x, x)$  can appear, for example, in the one loop  $\mathcal{O}(\lambda)$  bubble self energy or one loop  $\mathcal{O}(\beta)$  tadpole. Accordingly, the divergence can be canceled respectively by the one loop mass renormalisation and the one loop tadpole counterterms,

$$\delta m_\lambda^2 = -\frac{\lambda H^{2-\epsilon}\Gamma(2-\epsilon)}{2^{3-\epsilon}\pi^{2-\epsilon/2}\Gamma(1-\epsilon/2)\epsilon} \quad \alpha = -\frac{\beta H^{2-\epsilon}\Gamma(2-\epsilon)}{2^{3-\epsilon}\pi^{2-\epsilon/2}\Gamma(1-\epsilon/2)\epsilon} \quad (11)$$

We also note for our purpose the square of the Feynman propagator

$$\begin{aligned}i\Delta_{++}^2(x, x') &= -\frac{i\mu^{-\epsilon}a'^{-4+2\epsilon}\Gamma(1-\epsilon/2)}{2^3\pi^{2-\epsilon/2}\epsilon(1-\epsilon)}\delta^d(x-x') + \frac{H^4}{2^6\pi^4}\ln^2\frac{\sqrt{\epsilon}H^2\Delta x_{++}^2}{4} - \frac{H^2(aa')^{-1}\ln\frac{\sqrt{\epsilon}H^2\Delta x_{++}^2}{4}}{2^4\pi^4\Delta x_{++}^2} \\ &\equiv -\frac{i\mu^{-\epsilon}a'^{-4+2\epsilon}\Gamma(1-\epsilon/2)}{2^3\pi^{2-\epsilon/2}\epsilon(1-\epsilon)}\delta^d(x-x') + \Phi_{\text{NL}}^{++}(x, x')\end{aligned}\quad (12)$$

where we have abbreviated all the non-local terms as  $\Phi_{\text{NL}}^{++}(x, x')$ . The square of the anti-Feynman propagator is just the complex conjugation of the above. On the other hand for the mixed kind of propagators, the local term containing the  $\delta$ -function will be absent. Eq. (12) can appear, for example, in the one loop  $\mathcal{O}(\beta^2)$  self energy contribution. The divergence can be absorbed by the mass renormalisation counterterm

$$\delta m_\beta^2 = \frac{\beta^2\mu^{-\epsilon}\Gamma(1-\epsilon/2)}{2^4\pi^{2-\epsilon/2}\epsilon(1-\epsilon)} \quad (13)$$

With these ingredients, we are ready to go into computing the loop corrections to the quartic and cubic vertex functions.

## 3 Loop correction to the four point vertex

### 3.1 One loop

The quartic vertex function at tree and one loop level is depicted in Fig. 1, e.g. [71]. Since we are only interested about the purely local part of the vertex functions, and the mixed kind of propagators do not have any purely local part (Section 2), we shall deal only with the Feynman propagators.

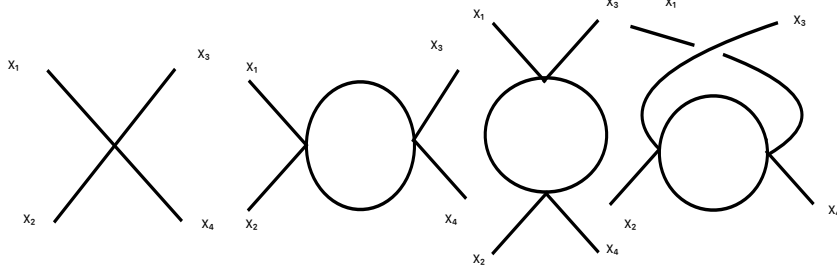


Figure 1: *Quartic vertex at tree and one loop level. The three one loop diagrams correspond to the three channels,  $s$ ,  $t$  and  $u$ . The one loop vertex is renormalised by one loop vertex renormalisation counterterm. For each channel, the counterterm is equal. See main text for discussion.*

The tree level amputated 4-point vertex can simply be read from Eq. (5),

$$-iV_+(x_1, x_2, x_3, x_4)|_{\text{Tree}} = -i(\lambda + \delta\lambda)a_1^d \delta^d(x_1 - x_2)\delta^d(x_1 - x_3)\delta^d(x_1 - x_4) \quad (14)$$

The one loop correction to the 4-point vertex was computed earlier in [21]

$$\begin{aligned} -iV_+(x_1, x_2, x_3, x_4)|_{1\text{loop}} = & -\frac{\lambda^2}{2} [(a_1 a_2)^d i\Delta_{++}^2(x_1, x_2)\delta^d(x_1 - x_4)\delta^d(x_2 - x_3) \\ & + (a_1 a_3)^d i\Delta_{++}^2(x_1, x_3)\delta^d(x_1 - x_2)\delta^d(x_3 - x_4) + (a_1 a_4)^d i\Delta_{++}^2(x_1, x_4)\delta^d(x_1 - x_3)\delta^d(x_2 - x_4)] \end{aligned} \quad (15)$$

Substituting now Eq. (12) into the above expression, we have after a little algebra

$$\begin{aligned} -iV_+(x_1, x_2, x_3, x_4)|_{1\text{loop}} = & \frac{3i\mu^{-\epsilon}\lambda^2}{2^4\pi^{2-\epsilon/2}} \frac{\Gamma(1-\epsilon/2)}{(1-\epsilon)\epsilon} a_1^{4-\epsilon+\epsilon} \delta^d(x_1 - x_2)\delta^d(x_1 - x_3)\delta^d(x_1 - x_4) \\ & -\frac{\lambda^2}{2} [(a_1 a_2)^4 \Phi_{\text{NL}}^{+++}(x_1, x_2)\delta^4(x_1 - x_4)\delta^4(x_2 - x_3) \\ & + (a_1 a_3)^4 \Phi_{\text{NL}}^{+++}(x_1, x_3)\delta^4(x_1 - x_2)\delta^4(x_3 - x_4) + (a_1 a_4)^4 \Phi_{\text{NL}}^{+++}(x_1, x_4)\delta^4(x_1 - x_3)\delta^4(x_2 - x_4)] \\ = & \frac{3i\mu^{-\epsilon}\lambda^2}{2^4\pi^{2-\epsilon/2}} \frac{\Gamma(1-\epsilon/2)}{(1-\epsilon)\epsilon} a_1^d \delta^d(x_1 - x_2)\delta^d(x_1 - x_3)\delta^d(x_1 - x_4) + \frac{3i\lambda^2}{2^4\pi^2} a_1^4 \ln a_1 \delta^4(x_1 - x_2)\delta^4(x_1 - x_3)\delta^4(x_1 - x_4) \\ & -\frac{\lambda^2}{2} [(a_1 a_2)^4 \Phi_{\text{NL}}^{+++}(x_1, x_2)\delta^4(x_1 - x_4)\delta^4(x_2 - x_3) \\ & + (a_1 a_3)^4 \Phi_{\text{NL}}^{+++}(x_1, x_3)\delta^4(x_1 - x_2)\delta^4(x_3 - x_4) + (a_1 a_4)^4 \Phi_{\text{NL}}^{+++}(x_1, x_4)\delta^4(x_1 - x_3)\delta^4(x_2 - x_4)] \end{aligned} \quad (16)$$

Comparing Eq. (14) and Eq. (16), we identify the one loop vertex counterterm

$$\delta\lambda^{(1)} = \delta\lambda_s^{(1)} + \delta\lambda_t^{(1)} + \delta\lambda_u^{(1)} = \frac{3\mu^{-\epsilon}\lambda^2}{2^4\pi^{2-\epsilon/2}} \frac{\Gamma(1-\epsilon/2)}{(1-\epsilon)\epsilon} \quad (17)$$

where the suffixes  $s$ ,  $t$  and  $u$  represent the three Mandelstam channels with  $\delta\lambda_s^{(1)} = \delta\lambda_t^{(1)} = \delta\lambda_u^{(1)}$ , so that we have the

renormalised result at one loop

$$\begin{aligned}
-iV_+(x_1, x_2, x_3, x_4)|_{1\text{ loop, Ren.}} &= \frac{3i\lambda^2}{2^4\pi^2} a_1^4 \ln a_1 \delta^4(x_1 - x_2) \delta^4(x_1 - x_3) \delta^4(x_1 - x_4) \\
&- \frac{\lambda^2}{2} [(a_1 a_2)^4 \Phi_{\text{NL}}^{++}(x_1, x_2) \delta^4(x_1 - x_4) \delta^4(x_2 - x_3) \\
&+ (a_1 a_3)^4 \Phi_{\text{NL}}^{++}(x_1, x_3) \delta^4(x_1 - x_2) \delta^4(x_3 - x_4) + (a_1 a_4)^4 \Phi_{\text{NL}}^{++}(x_1, x_4) \delta^4(x_1 - x_3) \delta^4(x_2 - x_4)] \quad (18)
\end{aligned}$$

Setting the scale factor to unity reproduces the result of the flat spacetime, in which case no secular effect can be present. Thus the purely local and renormalised vertex function found here can have no  $\Lambda = 0$  analogue. Let us now compute the two loop corrected vertex function.

### 3.2 Two loop

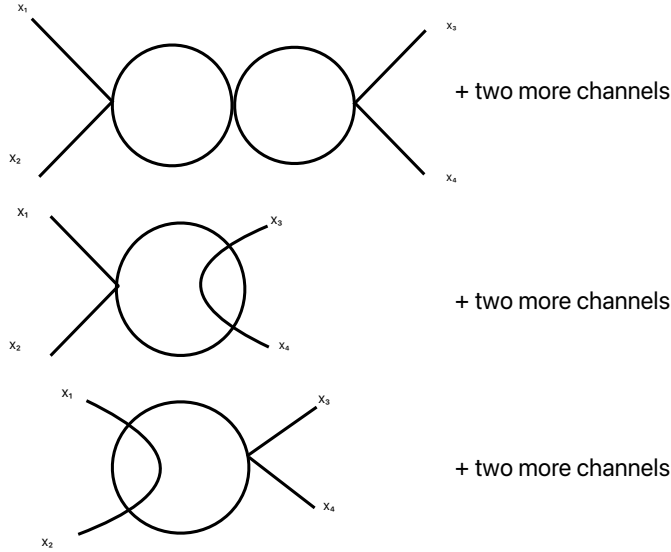


Figure 2: *Quartic vertex at two loop due to quartic self interaction. A diagram in any row has three channels, e.g. [71]. We have not considered the two loop diagrams at  $\mathcal{O}(\lambda^2\beta^2)$  containing internal cubic vertices, as they do not give any purely local contribution to the vertex functions. Likewise, the first diagram of Fig. 7 does not also yield any purely local contributions. See main text for discussion.*

The relevant Feynman diagrams for two loop correction to the vertex function due to the quartic self interaction are depicted in Fig. 2. There is another two loop  $\mathcal{O}(\lambda^3)$  diagram (the first of Fig. 7), which we have not considered here, as it does not yield any purely local correction to the four point vertex function. Let us now compute the first row of Fig. 2,

$$\begin{aligned}
-iV_+(x_1, x_2, x_3, x_4)|_{2\text{ loop}}^{(1)} &= \frac{i\lambda^3 a_1^d}{2^2} \int d^d x a^d [a_3^d i\Delta_{++}^2(x_1, x) i\Delta_{++}^2(x, x_3) \delta^d(x_1 - x_2) \delta^d(x_3 - x_4) \\
&+ a_4^d i\Delta_{++}^2(x_1, x) i\Delta_{++}^2(x, x_2) \delta^d(x_1 - x_3) \delta^d(x_2 - x_4) + a_2^d i\Delta_{++}^2(x_1, x) i\Delta_{++}^2(x, x_3) \delta^d(x_1 - x_4) \delta^d(x_2 - x_3)] \quad (19)
\end{aligned}$$

Substituting as earlier Eq. (12) into Eq. (19), we have

$$\begin{aligned}
-iV_+(x_1, x_2, x_3, x_4)|_{2\text{loop}}^{(1)} &= -\frac{3i\lambda^3\mu^{-2\epsilon}\Gamma^2(1-\epsilon/2)}{2^8\pi^{4-\epsilon}(1-\epsilon)^2}a_1^d\delta^d(x_1-x_2)\delta^d(x_1-x_3)\delta^d(x_1-x_4)\left(\frac{1}{\epsilon^2}+\frac{2\ln a_1}{\epsilon}\right) \\
&+ \frac{\mu^{-\epsilon}\lambda^3\Gamma(1-\epsilon/2)}{2^4\pi^{2-\epsilon/2}\epsilon(1-\epsilon)}\left[(a_1a_3)^d\Phi_{\text{NL}}^{++}(x_1, x_3)\delta^d(x_1-x_2)\delta^d(x_3-x_4)+(a_1a_4)^d\Phi_{\text{NL}}^{++}(x_1, x_4)\delta^d(x_1-x_3)\delta^d(x_2-x_4)\right. \\
&+ (a_1a_2)^d\Phi_{\text{NL}}^{++}(x_1, x_2)\delta^d(x_1-x_4)\delta^d(x_2-x_3)] - \frac{3i\lambda^3}{2^7\pi^4}a_1^4\ln^2 a_1\delta^4(x_1-x_2)\delta^4(x_1-x_3)\delta^4(x_1-x_4) \\
&+ \frac{\lambda^3}{2^5\pi^2}\left[(a_1a_3)^4\ln(a_1a_3)\Phi_{\text{NL}}^{++}(x_1, x_3)\delta^4(x_1-x_2)\delta^4(x_3-x_4)+(a_1a_4)^4\ln(a_1a_4)\Phi_{\text{NL}}^{++}(x_1, x_4)\delta^4(x_1-x_3)\delta^4(x_2-x_4)\right. \\
&+ (a_1a_2)^4\ln(a_1a_2)\Phi_{\text{NL}}^{++}(x_1, x_2)\delta^4(x_1-x_4)\delta^4(x_2-x_3)] \\
&+ \frac{i\lambda^3a_1^4}{2^2}\int d^4xa^4\left[a_3^4\Phi_{\text{NL}}^{++}(x_1, x)\Phi_{\text{NL}}^{++}(x, x_3)\delta^4(x_1-x_2)\delta^4(x_3-x_4)\right. \\
&+ a_4^4\Phi_{\text{NL}}^{++}(x_1, x)\Phi_{\text{NL}}^{++}(x, x_2)\delta^4(x_1-x_3)\delta^4(x_2-x_4)+a_2^4\Phi_{\text{NL}}^{++}(x_1, x)\Phi_{\text{NL}}^{++}(x, x_3)\delta^4(x_1-x_4)\delta^4(x_2-x_3)] \quad (20)
\end{aligned}$$

We now add with it the one loop vertex counterterm diagrams. We need to distinguish between the different channels here. From Eq. (17), we have

$$\begin{aligned}
-iV_+(x_1, x_2, x_3, x_4)|_{\text{CT}} &= -\lambda\left[\delta\lambda_s(a_1a_2)^d i\Delta_{++}^2(x_1, x_2)\delta^d(x_1-x_4)\delta^d(x_2-x_3)\right. \\
&+ \delta\lambda_t(a_1a_3)^d i\Delta_{++}^2(x_1, x_3)\delta^d(x_1-x_2)\delta^d(x_3-x_4)+\delta\lambda_u(a_1a_4)^d i\Delta_{++}^2(x_1, x_4)\delta^d(x_1-x_3)\delta^d(x_2-x_4)] \\
&= \frac{3i\mu^{-2\epsilon}\lambda^3\Gamma^2(1-\epsilon/2)}{2^7\pi^{4-\epsilon}(1-\epsilon)^2}a_1^d\left[\frac{1}{\epsilon^2}+\frac{\ln a_1}{\epsilon}+\frac{\ln^2 a_1}{2}\right]\delta^d(x_1-x_2)\delta^d(x_1-x_3)\delta^d(x_1-x_4) \\
&- \frac{\mu^{-\epsilon}\lambda^3\Gamma(1-\epsilon/2)}{2^4\pi^{2-\epsilon/2}(1-\epsilon)\epsilon}\left[(a_1a_2)^d\Phi_{\text{NL}}^{++}(x_1, x_2)\delta^d(x_1-x_4)\delta^d(x_2-x_3)+(a_1a_3)^d\Phi_{\text{NL}}^{++}(x_1, x_3)\delta^d(x_1-x_2)\delta^d(x_3-x_4)\right. \\
&+ (a_1a_4)^d\Phi_{\text{NL}}^{++}(x_1, x_4)\delta^d(x_1-x_3)\delta^d(x_2-x_4)] \quad (21)
\end{aligned}$$

Adding the above with Eq. (20), we have

$$\begin{aligned}
-iV_+(x_1, x_2, x_3, x_4)|_{2\text{loop}}^{(1)} &= \frac{3i\mu^{-2\epsilon}\lambda^3\Gamma^2(1-\epsilon/2)}{2^8\pi^{4-\epsilon}(1-\epsilon)^2\epsilon^2}a_1^d\delta^d(x_1-x_2)\delta^d(x_1-x_3)\delta^d(x_1-x_4) \\
&- \frac{3i\lambda^3}{2^8\pi^4}a_1^4\ln^2 a_1\delta^4(x_1-x_2)\delta^4(x_1-x_3)\delta^4(x_1-x_4)+\frac{\lambda^3}{2^5\pi^2}\left[(a_1a_3)^4\ln(a_1a_3)\Phi_{\text{NL}}^{++}(x_1, x_3)\delta^4(x_1-x_2)\delta^4(x_3-x_4)\right. \\
&+ (a_1a_4)^4\ln(a_1a_4)\Phi_{\text{NL}}^{++}(x_1, x_4)\delta^4(x_1-x_3)\delta^4(x_2-x_4)+(a_1a_2)^4\ln(a_1a_2)\Phi_{\text{NL}}^{++}(x_1, x_2)\delta^4(x_1-x_4)\delta^4(x_2-x_3)] \\
&+ \frac{i\lambda^3a_1^4}{2^2}\int d^4xa^4\left[a_3^4\Phi_{\text{NL}}^{++}(x_1, x)\Phi_{\text{NL}}^{++}(x, x_3)\delta^4(x_1-x_2)\delta^4(x_3-x_4)\right. \\
&+ a_4^4\Phi_{\text{NL}}^{++}(x_1, x)\Phi_{\text{NL}}^{++}(x, x_2)\delta^4(x_1-x_3)\delta^4(x_2-x_4)+a_2^4\Phi_{\text{NL}}^{++}(x_1, x)\Phi_{\text{NL}}^{++}(x, x_3)\delta^4(x_1-x_4)\delta^4(x_2-x_3)] \quad (22)
\end{aligned}$$

We shall renormalise the divergence in the first line after we compute the two other two loop vertex diagrams of Fig. 2. Note also that we have additional divergent terms due to the secular logarithms compared to the flat spacetime in Eq. (20). Those additional divergences are taken care of by the additional divergent terms of the counterterm contribution, Eq. (21).



The second row of Fig. 2 reads

$$\begin{aligned}
-iV_+(x_1, x_2, x_3, x_4)|_{2\text{loop}}^{(2)} &= \frac{i\lambda^3 a_1^d}{2} [(a_2 a_3)^d i\Delta_{++}(x_1, x_3) i\Delta_{++}(x_1, x_2) i\Delta_{++}^2(x_2, x_3) \delta^d(x_1 - x_4) \\
&+ (a_3 a_4)^d i\Delta_{++}(x_1, x_3) i\Delta_{++}(x_1, x_4) i\Delta_{++}^2(x_3, x_4) \delta^d(x_1 - x_2) + (a_4 a_2)^d i\Delta_{++}(x_1, x_2) i\Delta_{++}(x_1, x_4) i\Delta_{++}^2(x_2, x_4) \delta^d(x_1 - x_3)]
\end{aligned} \tag{23}$$

Substituting Eq. (12) into the above expression, we obtain

$$\begin{aligned}
-iV_+(x_1, x_2, x_3, x_4)|_{2\text{loop}, \text{loc}}^{(2)} &= -\frac{3i\lambda^3 \mu^{-2\epsilon} \Gamma^2(1 - \epsilon/2)}{2^7 \pi^{4-\epsilon} (1 - \epsilon)^2} a_1^d \delta^d(x_1 - x_2) \delta^d(x_1 - x_3) \delta^d(x_1 - x_4) \left( \frac{1}{\epsilon^2} + \frac{2 \ln a_1}{\epsilon} \right) \\
&- \frac{3i\lambda^3}{2^6 \pi^4} a_1^4 \ln^2 a_1 \delta^4(x_1 - x_2) \delta^4(x_1 - x_3) \delta^4(x_1 - x_4) + \frac{\mu^{-\epsilon} \lambda^3 \Gamma(1 - \epsilon/2)}{2^3 \pi^{2-\epsilon/2} \epsilon (1 - \epsilon)} [(a_1 a_3)^d \Phi_{\text{NL}}^{++}(x_1, x_3) \delta^d(x_2 - x_3) \delta^d(x_1 - x_4) \\
&+ (a_1 a_4)^d \Phi_{\text{NL}}^{++}(x_1, x_4) \delta^d(x_1 - x_2) \delta^d(x_3 - x_4) + (a_1 a_2)^d \Phi_{\text{NL}}^{++}(x_1, x_2) \delta^d(x_1 - x_3) \delta^d(x_2 - x_4)] \\
&+ \frac{\lambda^3}{2^3 \pi^2} [(a_1 a_3)^4 \ln a_3 \Phi_{\text{NL}}^{++}(x_1, x_3) \delta^4(x_2 - x_3) \delta^4(x_1 - x_4) \\
&+ (a_1 a_4)^4 \ln a_4 \Phi_{\text{NL}}^{++}(x_1, x_4) \delta^4(x_1 - x_2) \delta^4(x_3 - x_4) + (a_1 a_2)^4 \ln a_2 \Phi_{\text{NL}}^{++}(x_1, x_2) \delta^4(x_1 - x_3) \delta^4(x_2 - x_4)] \\
&+ \frac{i\lambda^3 a_1^4}{2} [(a_2 a_3)^4 \Phi_{\text{NL}}^{++}(x_1, x_3) \Phi_{\text{NL}}^{++}(x_2, x_3) \delta^4(x_1 - x_4) + (a_3 a_4)^4 \Phi_{\text{NL}}^{++}(x_1, x_3) \Phi_{\text{NL}}^{++}(x_3, x_4) \delta^4(x_1 - x_2) \\
&+ (a_4 a_1)^4 \Phi_{\text{NL}}^{++}(x_2, x_1) \Phi_{\text{NL}}^{++}(x_1, x_4) \delta^4(x_2 - x_3)]
\end{aligned} \tag{24}$$

A clarification is in order here. Since each of the channels contains two  $\delta$ -functions, the channels are obtained only when we encounter a square of the propagator. Thus in order to obtain the full channel wise contributions, for example for the first term on the right hand side of Eq. (23) we must take into account the effect when  $x_2 \rightarrow x_3$ , in the product  $i\Delta_{++}(x_1, x_3) i\Delta_{++}(x_1, x_2)$ . Ignoring this still gives a channel structure, however the respective contributions become half, which is incomplete. As in the flat spacetime [71], the above diagram is renormalised by adding with it the  $(s+t)$ -counterterm contributions, Eq. (17), plus two more channels (corresponding to  $(t+u)$  and  $(u+s)$  counterterms), which is just twice of Eq. (21). Adding this with Eq. (24), we obtain the contribution free from any  $\ln a/\epsilon$ -type divergences,

$$\begin{aligned}
-iV_+(x_1, x_2, x_3, x_4)|_{2\text{loop}}^{(2)} &= \frac{3i\lambda^3 \mu^{-2\epsilon} \Gamma^2(1 - \epsilon/2)}{2^7 \pi^{4-\epsilon} (1 - \epsilon)^2 \epsilon^2} a_1^d \delta^d(x_1 - x_2) \delta^d(x_1 - x_3) \delta^d(x_1 - x_4) \\
&- \frac{3i\lambda^3}{2^7 \pi^4} a_1^4 \ln^2 a_1 \delta^4(x_1 - x_2) \delta^4(x_1 - x_3) \delta^4(x_1 - x_4) + \frac{\lambda^3}{2^3 \pi^2} [(a_1 a_3)^4 \ln a_3 \Phi_{\text{NL}}^{++}(x_1, x_3) \delta^4(x_2 - x_3) \delta^4(x_1 - x_4) \\
&+ (a_1 a_4)^4 \ln a_4 \Phi_{\text{NL}}^{++}(x_1, x_4) \delta^4(x_1 - x_2) \delta^4(x_3 - x_4) + (a_1 a_2)^4 \ln a_2 \Phi_{\text{NL}}^{++}(x_1, x_2) \delta^4(x_1 - x_3) \delta^4(x_2 - x_4)] \\
&+ \frac{i\lambda^3 a_1^4}{2} [(a_2 a_3)^4 \Phi_{\text{NL}}^{++}(x_1, x_3) \Phi_{\text{NL}}^{++}(x_2, x_3) \delta^4(x_1 - x_4) + (a_3 a_4)^4 \Phi_{\text{NL}}^{++}(x_1, x_3) \Phi_{\text{NL}}^{++}(x_3, x_4) \delta^4(x_1 - x_2) \\
&+ (a_4 a_1)^4 \Phi_{\text{NL}}^{++}(x_2, x_1) \Phi_{\text{NL}}^{++}(x_1, x_4) \delta^4(x_2 - x_3)]
\end{aligned} \tag{25}$$

Finally, the third row of Fig. 2 reads

$$\begin{aligned}
-iV_+(x_1, x_2, x_3, x_4)|_{2\text{loop}}^{(3)} &= \frac{i\lambda^3 a_2^d}{2} [(a_1 a_3)^d i\Delta_{++}(x_2, x_3) i\Delta_{++}(x_2, x_1) i\Delta_{++}^2(x_1, x_3) \delta^d(x_2 - x_4) \\
&+ (a_3 a_4)^d i\Delta_{++}(x_2, x_3) i\Delta_{++}(x_2, x_4) i\Delta_{++}^2(x_3, x_4) \delta^d(x_2 - x_1) + (a_4 a_1)^d i\Delta_{++}(x_2, x_1) i\Delta_{++}(x_2, x_4) i\Delta_{++}^2(x_1, x_4) \delta^d(x_2 - x_3)]
\end{aligned} \tag{26}$$

The analogue of Eq. (25) in this case can be derived in a likewise manner

$$\begin{aligned}
-iV_+(x_1, x_2, x_3, x_4)|_{2\text{loop, loc}}^{(3)} &= \frac{3i\lambda^3\mu^{-2\epsilon}\Gamma^2(1-\epsilon/2)}{2^7\pi^{4-\epsilon}(1-\epsilon)^2\epsilon^2} a_2^d \delta^d(x_2-x_1)\delta^d(x_2-x_3)\delta^d(x_2-x_4) \\
&- \frac{3i\lambda^3}{2^7\pi^4} a_2^4 \ln^2 a_2 \delta^4(x_2-x_1)\delta^4(x_2-x_3)\delta^4(x_2-x_4) + \frac{\lambda^3}{2^3\pi^2} [(a_2 a_3)^4 \ln a_3 \Phi_{\text{NL}}(x_2, x_3) \delta^4(x_1-x_3) \delta^4(x_2-x_4) \\
&+ (a_2 a_4)^4 \ln a_4 \Phi_{\text{NL}}(x_2, x_4) \delta^4(x_2-x_1) \delta^4(x_3-x_4) + (a_2 a_1)^4 \ln a_1 \Phi_{\text{NL}}(x_2, x_1) \delta^4(x_2-x_3) \delta^4(x_1-x_4)] \\
&+ \frac{i\lambda^3 a_1^4}{2} [(a_2 a_3)^4 \Phi_{\text{NL}}^{++}(x_1, x_3) \Phi_{\text{NL}}^{++}(x_2, x_3) \delta^4(x_2-x_4) + (a_3 a_4)^4 \Phi_{\text{NL}}^{++}(x_2, x_3) \Phi_{\text{NL}}^{++}(x_3, x_4) \delta^4(x_2-x_1) \\
&+ (a_4 a_2)^4 \Phi_{\text{NL}}^{++}(x_2, x_1) \Phi_{\text{NL}}^{++}(x_1, x_4) \delta^4(x_2-x_3)] \tag{27}
\end{aligned}$$

Note by comparison of the above with Eq. (24) that these purely local parts are not really different by the virtue of the  $\delta$ -functions, as expected, and one can be obtained from the other by purely making the interchange  $x_1 \leftrightarrow x_2$ . However, we have kept them in a little bit different appearances just to emphasise the different topologies of the corresponding diagrams.

Combining now Eq. (27), Eq. (25) and Eq. (22), we find the only remaining two loop divergent term for Fig. 2 to be

$$-iV_+(x_1, x_2, x_3, x_4)|_{2\text{loop, div}}^{(3)} = 3 \times \frac{5i\lambda^3\mu^{-2\epsilon}\Gamma^2(1-\epsilon/2)}{2^8\pi^{4-\epsilon}(1-\epsilon)^2\epsilon^2} a_1^d \delta^d(x_1-x_2)\delta^d(x_1-x_3)\delta^d(x_1-x_4) \tag{28}$$

which leads to the two loop quartic vertex counterterm,

$$\delta\lambda^{(2)} = \delta\lambda_s^{(2)} + \delta\lambda_t^{(2)} + \delta\lambda_u^{(2)}, \quad \delta\lambda_s^{(2)} = \delta\lambda_t^{(2)} = \delta\lambda_u^{(2)} = \frac{5\lambda^3\mu^{-2\epsilon}\Gamma^2(1-\epsilon/2)}{2^8\pi^{4-\epsilon}(1-\epsilon)^2\epsilon^2} \tag{29}$$

which completely renormalises the addition of Eq. (27), Eq. (25) and Eq. (22). Since we are interested only about the purely local vertex function, we pick up the term

$$-iV_+(x_1, x_2, x_3, x_4)|_{2\text{loop, loc, Ren}} = -\frac{15i\lambda^3}{2^8\pi^4} a_1^4 \ln^2 a_1 \delta^4(x_1-x_2)\delta^4(x_1-x_3)\delta^4(x_1-x_4) \tag{30}$$

Combining the above with Eq. (18) and Eq. (14), we have the purely local, renormalised contribution to the 4-point vertex function up to two loop

$$-iV_+(x_1, x_2, x_3, x_4)|_{\text{loc, Ren}} = -\left[\lambda - \frac{3\lambda^2}{2^4\pi^2} \ln a_1 + \frac{15\lambda^3}{2^8\pi^4} \ln^2 a_1\right] ia_1^4 \delta^4(x_1-x_2)\delta^4(x_1-x_3)\delta^4(x_1-x_4) + \mathcal{O}(\lambda^4) \tag{31}$$

which leads to a natural decomposition,

$$-iV_+(x_1, x_2, x_3, x_4)|_{\text{loc, Ren}} \equiv -ia_1^4 \delta^4(x_1-x_2)\delta^4(x_1-x_3)\delta^4(x_1-x_4) \times \lambda_{\text{eff, loc}}(a_1) \tag{32}$$

where the spatially homogeneous local vertex function  $\lambda_{\text{eff, loc}}(a_1)$  contains the secular logarithms

$$\lambda_{\text{eff, loc}}(a) := \lambda - \frac{3\lambda^2}{2^4\pi^2} \ln a + \frac{15\lambda^3}{2^8\pi^4} \ln^2 a + \mathcal{O}(\lambda^4) \tag{33}$$

The appearances of the secular logarithm terms clearly indicates the breakdown of the perturbation theory at sufficiently late times. This also shows the necessity of resummation, which we wish to pursue in Section 5.

In [Appendix A](#), we have sketched the computation of the other  $\mathcal{O}(\lambda^3)$  diagram, which does not yield any purely local contribution to the vertex function. Note also that contribution from such diagram is vanishing in flat spacetime, once we renormalise it. However in the de Sitter spacetime, as we have discussed in [Appendix A](#), the renormalised expression is non-vanishing, owing to the secular logarithm. We now wish to do similar computations for the cubic vertex function in the presence of a quartic self interaction. The loop correction due to the cubic self interaction alone does not yield any purely local contribution to the 3-point vertex function.

## 4 Loop correction to the cubic vertex function

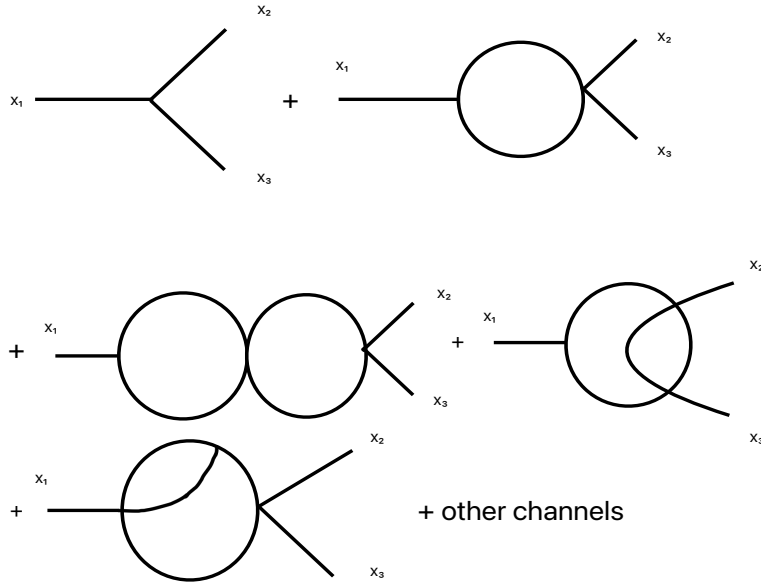


Figure 3: Cubic vertex function up to two loop for a cubic plus quartic self interaction. We have not considered corrections due to the cubic self interaction itself, for any such diagram does not yield any purely local contribution. We have also discussed another diagram in [Fig. 7 \(Appendix A\)](#) in the presence of quartic plus cubic coupling. Although this particular diagram does not produce any purely local contribution, it has a non-vanishing renormalised (non-local) contribution by the virtue of secular logarithms. Such non-vanishing contribution is not possible in the flat spacetime. See main text for discussion.

The cubic vertex function at tree, one loop and two loop level has been depicted in [Fig. 3](#), respectively at  $\mathcal{O}(\beta)$ ,  $\mathcal{O}(\lambda\beta)$  and  $\mathcal{O}(\lambda^2\beta)$  and have discarded the diagrams which do not make any purely local contribution to the cubic vertex function. We have considered another  $\mathcal{O}(\lambda^2\beta)$  diagram in [Appendix A](#), [Fig. 7](#). Although this diagram does not contribute to purely local vertex functions, we have addressed it in order emphasise that it has a non-vanishing renormalised expression via the secular logarithm. In the flat spacetime however, this diagram vanishes after renormalisation.

The tree level cubic vertex is given by the first of [Fig. 3](#) and [Eq. \(5\)](#),

$$-iV_+(x_1, x_2, x_3) = -i(\beta + \delta\beta)a_1^d\delta^d(x_1 - x_2)\delta^d(x_1 - x_3) \quad (34)$$

## 4.1 One loop

The one loop correction to the cubic vertex due to the quartic self interaction, given by the second of Fig. 3, reads

$$\begin{aligned}
-iV_+(x_1, x_2, x_3)|_{1\text{ loop}} &= -\frac{\lambda\beta}{2} [(a_1 a_3)^d i\Delta_{++}^2(x_1, x_3) \delta^d(x_1 - x_2) \\
&+ (a_1 a_2)^d i\Delta_{++}^2(x_1, x_2) \delta^d(x_1 - x_3) + (a_1 a_3)^d i\Delta_{++}^2(x_3, x_1) \delta^d(x_2 - x_3)] \\
&= \frac{3i\mu^{-\epsilon} \lambda\beta \Gamma(1 - \epsilon/2)}{2^4 \pi^{2-\epsilon/2} \epsilon(1 - \epsilon)} a_1^d \delta^d(x_1 - x_3) \delta^d(x_1 - x_2) + \frac{3i\lambda\beta}{2^4 \pi^2} a_1^4 \ln a_1 \delta^4(x_1 - x_3) \delta^4(x_1 - x_2) \\
&- \frac{\lambda\beta}{2} [(a_1 a_3)^4 \Phi_{\text{NL}}^{++}(x_1, x_3) \delta^4(x_1 - x_2) + (a_1 a_2)^4 \Phi_{\text{NL}}^{++}(x_1, x_2) \delta^d(x_1 - x_3) + (a_1 a_3)^4 \Phi_{\text{NL}}^{++}(x_3, x_1) \delta^d(x_2 - x_3)] \quad (35)
\end{aligned}$$

where as earlier, we have substituted Eq. (12).

The one loop cubic vertex counterterm for different channels can then be read off from Eq. (34),

$$\delta\beta_{1\text{ loop}} = (\delta\beta_s + \delta\beta_t + \delta\beta_u)_{1\text{ loop}} = \frac{3\mu^{-\epsilon} \lambda\beta \Gamma(1 - \epsilon/2)}{2^4 \pi^{2-\epsilon/2} \epsilon(1 - \epsilon)} \quad (36)$$

Note that as of the pure quartic self interaction discussed in the preceding section, the different channels' contribution to the counterterm is the same. We now note down for our present purpose the purely local renormalised cubic vertex function at one loop,

$$-iV_+(x_1, x_2, x_3)|_{1\text{ loop, loc, Ren.}} = \frac{3i\lambda\beta}{2^4 \pi^2} a_1^4 \ln a_1 \delta^4(x_1 - x_3) \delta^4(x_1 - x_2) \quad (37)$$

As we have stated earlier, the  $\mathcal{O}(\beta^3)$  one loop contribution has no purely local part, and hence will not be considered here for our present purpose.

## 4.2 Two loop

The two loop diagrams for the cubic vertex function which contribute to the purely local vertex function are given by the second and third row of Fig. 3. Diagram of each category contains three channels. The computations will be similar to that of the quartic vertex, discussed in the preceding section. The first two loop diagram of Fig. 3 reads

$$\begin{aligned}
-iV_+(x_1, x_2, x_3)|_{2\text{ loop}}^{(1)} &= \frac{i\lambda^2\beta}{2^2} \left[ (a_1 a_2)^d \int d^d x a^d i\Delta_{++}^2(x_1, x) i\Delta_{++}^2(x, x_2) \delta^d(x_2 - x_3) \right. \\
&+ (a_1 a_3)^d \int d^d x a^d i\Delta_{++}^2(x_1, x) i\Delta_{++}^2(x, x_2) \delta^d(x_1 - x_3) + (a_2 a_3)^d \int d^d x a^d i\Delta_{++}^2(x_1, x) i\Delta_{++}^2(x, x_3) \delta^d(x_1 - x_2) \left. \right] \\
&= \frac{i\lambda^2\beta}{2^2} \left[ -\frac{3\mu^{-2\epsilon} \Gamma^2(1 - \epsilon/2)}{2^6 \pi^{4-\epsilon} (1 - \epsilon)^2} a_1^d \delta^d(x_1 - x_2) \delta^d(x_1 - x_3) \left( \frac{1}{\epsilon^2} + \frac{2 \ln a_1}{\epsilon} + 2 \ln^2 a_1 \right) \right. \\
&- \frac{i\mu^{-\epsilon} \Gamma(1 - \epsilon/2)}{2^2 \pi^{2-\epsilon/2} \epsilon(1 - \epsilon)} ((a_1 a_2)^d \Phi_{\text{NL}}^{++}(x_1, x_2) \delta^d(x_2 - x_3) + (a_1 a_3)^d \Phi_{\text{NL}}^{++}(x_1, x_2) \delta^d(x_1 - x_3) + (a_2 a_3)^d \Phi_{\text{NL}}^{++}(x_2, x_3) \delta^d(x_1 - x_2)) \\
&- \frac{i(a_1 a_2)^4}{2^3 \pi^2} (\ln(a_1 a_2) \Phi_{\text{NL}}^{++}(x_1, x_2) \delta^4(x_2 - x_3) + \ln(a_3 a_2) \Phi_{\text{NL}}^{++}(x_3, x_2) \delta^4(x_1 - x_3) + \ln(a_1 a_3) \Phi_{\text{NL}}^{++}(x_1, x_3) \delta^4(x_1 - x_2)) \\
&+ \left( (a_1 a_2)^4 \int d^4 x a^4 \Phi_{\text{NL}}^{++}(x_1, x) \Phi_{\text{NL}}^{++}(x, x_2) \delta^4(x_2 - x_3) + (a_1 a_3)^4 \int d^4 x a^4 \Phi_{\text{NL}}^{++}(x_1, x) \Phi_{\text{NL}}^{++}(x, x_2) \delta^4(x_1 - x_3) \right. \\
&\left. + (a_2 a_3)^4 \int d^4 x a^4 \Phi_{\text{NL}}^{++}(x_1, x) \Phi_{\text{NL}}^{++}(x, x_3) \delta^4(x_1 - x_2) \right) \left. \right] \quad (38)
\end{aligned}$$

We add with the above the one loop counterterm contributions for different channels from Eq. (17), Eq. (36),

$$\begin{aligned}
-iV_+(x_1, x_2, x_3)|_{1\text{ loop CT}} &= -\frac{\beta\delta\lambda_s + \lambda\delta\beta_s}{2}(a_1a_3)^d i\Delta_{++}^2(x_1, x_3)\delta^d(x_1 - x_2) + t \text{ and } u \text{ channel contributions} \\
&= \frac{3i\mu^{-2\epsilon}\beta\lambda^2\Gamma^2(1-\epsilon/2)}{2^7\pi^{4-\epsilon}(1-\epsilon)^2}a_1^d\delta^d(x_1 - x_3)\delta^d(x_1 - x_2)\left(\frac{1}{\epsilon^2} + \frac{\ln a_1}{\epsilon} + \frac{\ln^2 a_1}{2}\right) \\
&\quad -\frac{\mu^{-\epsilon}\beta\lambda^2\Gamma(1-\epsilon/2)}{2^4\pi^{2-\epsilon/2}\epsilon(1-\epsilon)}\left[(a_1a_2)^d\Phi_{\text{NL}}^{++}(x_1, x_2)\delta^d(x_2 - x_3) + (a_1a_3)^d\Phi_{\text{NL}}^{++}(x_1, x_2)\delta^d(x_1 - x_3) + (a_2a_3)^d\Phi_{\text{NL}}^{++}(x_2, x_3)\delta^d(x_1 - x_2)\right]
\end{aligned} \tag{39}$$

so that the purely local part of Eq. (38) is given by

$$-iV_+(x_1, x_2, x_3)|_{2\text{ loop loc}}^{(1)} = -\frac{3i\mu^{-2\epsilon}\beta\lambda^2\Gamma^2(1-\epsilon/2)}{2^8\pi^{4-\epsilon}(1-\epsilon)^2}a_1^d\delta^d(x_1 - x_3)\delta^d(x_1 - x_2)\left(-\frac{1}{\epsilon^2} + \ln^2 a_1\right) \tag{40}$$

The next two loop diagram of Fig. 3 reads

$$\begin{aligned}
-iV_+(x_1, x_2, x_3)|_{2\text{ loop}}^{(2)} &= \frac{i\beta\lambda^2}{2}(a_1a_2a_3)^d\left[i\Delta_{++}(x_1, x_2)i\Delta_{++}(x_1, x_3)i\Delta_{++}^2(x_2, x_3) \right. \\
&\quad \left. + i\Delta_{++}(x_2, x_1)i\Delta_{++}(x_2, x_3)i\Delta_{++}^2(x_3, x_1) + i\Delta_{++}(x_3, x_1)i\Delta_{++}(x_3, x_2)i\Delta_{++}^2(x_1, x_2)\right] \\
&= -\frac{3i\mu^{-2\epsilon}\beta\lambda^2\Gamma^2(1-\epsilon/2)}{2^7\pi^{4-\epsilon}(1-\epsilon)^2}\left(\frac{1}{\epsilon^2} + \frac{2\ln a_1}{\epsilon} + 2\ln^2 a_1\right) + \frac{\mu^{-\epsilon}\beta\lambda^2\Gamma(1-\epsilon/2)}{2^3\pi^{2-\epsilon/2}\epsilon(1-\epsilon)}\left[(a_1a_2)^d\Phi_{\text{NL}}^{++}(x_1, x_2)\delta^d(x_2 - x_3) \right. \\
&\quad \left. + (a_2a_3)^d\Phi_{\text{NL}}^{++}(x_2, x_3)\delta^d(x_1 - x_3) + (a_3a_1)^d\Phi_{\text{NL}}^{++}(x_3, x_1)\delta^d(x_1 - x_2)\right] + \frac{\beta\lambda^2}{2^4\pi^2}\left[(a_1a_2)^4\ln(a_1a_2)\Phi_{\text{NL}}^{++}(x_1, x_2)\delta^4(x_2 - x_3) \right. \\
&\quad \left. + (a_2a_3)^4\ln(a_2a_3)\Phi_{\text{NL}}^{++}(x_2, x_3)\delta^4(x_1 - x_3) + (a_3a_1)^4\ln(a_1a_3)\Phi_{\text{NL}}^{++}(x_3, x_1)\delta^4(x_1 - x_2)\right] + \text{purely non-local terms}
\end{aligned} \tag{41}$$

where we have suppressed the purely non-local terms containing no  $\delta$ -functions, as for our present purpose they will not be necessary. All but the  $\mathcal{O}(\epsilon^{-2})$  divergence of Eq. (41) can be canceled as of Eq. (24) (corresponding to the second or third of Fig. 2), discussed in the preceding section. We have for the purely local part

$$-iV_+(x_1, x_2, x_3)|_{2\text{ loop loc}}^{(2)} = -\frac{3i\mu^{-2\epsilon}\beta\lambda^2\Gamma^2(1-\epsilon/2)}{2^7\pi^{4-\epsilon}(1-\epsilon)^2}a_1^d\delta^d(x_1 - x_3)\delta^d(x_1 - x_2)\left(-\frac{1}{\epsilon^2} + \ln^2 a_1\right) \tag{42}$$

The last two loop diagram of Fig. 3 for the cubic vertex reads,

$$-iV_+(x_1, x_2, x_3)|_{2\text{ loop}}^{(3)} = \frac{i\lambda^2\beta}{2}\left[(a_1a_2)^d\int d^d x a^d i\Delta_{++}^2(x_1, x)i\Delta_{++}(x, x_2)i\Delta_{++}(x_1, x_3)\delta^d(x_2 - x_3) + \text{two more channels}\right], \tag{43}$$

which can be evaluated as earlier to obtain the purely local contribution

$$-iV_+(x_1, x_2, x_3)|_{2\text{ loop, loc}}^{(3)} = -\frac{3i\mu^{-2\epsilon}\beta\lambda^2\Gamma^2(1-\epsilon/2)}{2^8\pi^{4-\epsilon}(1-\epsilon)^2}a_1^d\left(-\frac{1}{\epsilon^2} + \ln^2 a_1\right)\delta^d(x_1 - x_2)\delta^d(x_1 - x_3) \tag{44}$$

Combining now Eq. (40), Eq. (42) and Eq. (44), as well as introducing the two loop cubic vertex counterterm,

$$\delta\beta_{2\text{ loop}} = \delta\beta_{2\text{ loop}}^s + \delta\beta_{2\text{ loop}}^t + \delta\beta_{2\text{ loop}}^u = \frac{3\mu^{-2\epsilon}\beta\lambda^2\Gamma^2(1-\epsilon/2)}{2^6\pi^4-\epsilon\epsilon^2(1-\epsilon)^2}, \quad (45)$$

we finally obtain the purely local part of the renormalised cubic vertex function at two loop

$$-iV_+(x_1, x_2, x_3)|_{2\text{ loop, Ren., loc.}} = -\frac{3i\beta\lambda^2}{2^6\pi^4}a_1^4\ln^2 a_1\delta^4(x_1-x_2)\delta^4(x_1-x_3) \quad (46)$$

where as earlier, counterterm corresponding to each channel is equal.

Combining now Eq. (46) with Eq. (34) and Eq. (37), we have the renormalised expression for the purely local part of the cubic vertex function

$$-iV_+(x_1, x_2, x_3)|_{\text{Ren., loc.}} = \left(-i\beta + \frac{3i\lambda\beta}{2^4\pi^2}\ln a_1 - \frac{3i\beta\lambda^2}{2^6\pi^4}\ln^2 a_1 + \mathcal{O}(\beta\lambda^3)\right)a_1^4\delta^4(x_1-x_2)\delta^4(x_1-x_3) \quad (47)$$

As of the quartic case, Eq. (33), we identify now the effective spatially homogeneous cubic vertex function containing the secular logarithms,

$$\beta_{\text{eff, loc}}(a) = \beta - \frac{3\lambda\beta}{2^4\pi^2}\ln a + \frac{3\beta\lambda^2}{2^6\pi^4}\ln^2 a + \mathcal{O}(\beta\lambda^3) \quad (48)$$

We wish to emphasise once again that neither Eq. (33) nor Eq. (48) has any flat spacetime analogue ( $a = 1$ ). Also, neither of these perturbative results can be trusted after sufficiently large number of  $e$ -foldings, when the secular logarithm terms become large. Accordingly, we wish to attempt below obtaining non-perturbative expressions for these vertex functions, as follows.

## 5 Non-perturbative values of the vertex functions via the dynamical mass generation

The late time secular growth of  $\lambda_{\text{eff, loc}}(a)$  (Eq. (33)) and  $\beta_{\text{eff, loc}}(a)$  (Eq. (48)) corresponds to the massless minimally coupled scalar field residing in the loops. Such a scalar, as we have discussed in Section 2, cannot have any de Sitter invariant representation of the two point function. On the other hand if the field is massive, the corresponding two point functions are perfectly de Sitter invariant no matter how small the mass is, and hence no such secular effect can be present for a massive scalar. There have been several attempts in the literature to resum these large secular logarithms, chiefly in the context of the two point correlation function of the scalar field. Specifically, part of such secular logarithms arising from the local part of the self energy can be resummed using various methods to generate a dynamical mass of the scalar field at late times, e.g. [5, 38, 44, 45, 46, 47, 48, 49, 56, 53] (see also references therein). By the word ‘local’, we essentially refer to the part of the self energy that shrinks the corresponding loop and vertices to a single point. The dynamically generated late time mass guarantees that the de Sitter isometry can be retained at late times. We recall that the large temporal logarithms appearing in  $\lambda_{\text{eff, loc}}(a)$  or  $\beta_{\text{eff, loc}}(a)$  correspond to the purely local part of the loops. Hence it seems natural to expect that the vertex functions we have considered here will also acquire bounded, resummed non-perturbative values at late times, owing to the dynamical generation of the field mass, as follows.

From Eq. (10) we note that the renormalised value of the propagator at the coincidence limit is given by

$$i\Delta(x, x)|_{\text{Ren}} = \langle\phi^2(x)\rangle_{\text{Ren}} = \frac{H^2}{2^2\pi^2}\ln a \quad (49)$$

Substituting the above into Eq. (33), we have

$$\lambda_{\text{eff,loc}} = \lambda - \frac{3\lambda^2}{2^2 H^2} \langle \phi^2 \rangle + \frac{15\lambda^3}{2^4 H^4} \langle \phi^2 \rangle^2 + \mathcal{O}(\lambda^4) \quad (50)$$

It is well known that  $\langle \phi^2 \rangle$  can be resummed for a massless minimal scalar field with a quartic self interaction (corresponding to the local part of the scalar self energy) to yield a late time finite value given by [56]

$$\langle \phi^2 \rangle = \frac{\sqrt{3}H^2}{2\pi\sqrt{\lambda}} \quad (51)$$

For a massive and minimally coupled scalar, the Feynman propagator in the de Sitter spacetime reads

$$i\Delta_{++}(x, x', m) = \frac{H^2}{4\pi^2} \left( \frac{1}{y_{++}(x, x')} + \frac{1}{2} \ln y_{++}(x, x') + \frac{1}{2(3/2 - \nu)} \right) \quad (52)$$

where  $\nu = (9/4 - m^2/H^2)^{1/2}$  is a parameter and the complex distance function  $y_{++}(x, x')$  is given by Eq. (8), Eq. (9). Thus when  $m/H$  is small, we have at the leading order the regularised result

$$i\Delta_{++}(x, x, m)|_{\text{Ren.}} \equiv \langle \phi^2 \rangle = \frac{3H^4}{8\pi^2 m^2} \quad (53)$$

Comparing the above with the result of the massless scalar, Eq. (51), one concludes that the scalar acquires a dynamically generated mass at late times [66, 67]

$$\bar{m}_{\text{dyn}}^2 = \frac{\sqrt{3\lambda}}{4\pi} \quad (54)$$

where  $\bar{m}_{\text{dyn}} = m_{\text{dyn}}/H$  is dimensionless. For our purpose, we also need the extension of the above result for quartic plus cubic self interaction potential, given by the real positive root of the cubic equation [52, 54],

$$(\bar{m}_{\text{dyn}}^2)^3 = \frac{6\lambda - 3\bar{\beta}^2}{32\pi^2} \bar{m}_{\text{dyn}}^2 - \frac{18\lambda^2 - 27\lambda\bar{\beta}^2}{512\pi^4} \quad (55)$$

where  $\bar{\beta} = \beta/H$  is dimensionless. It is easy to see that setting  $\bar{\beta} = 0$  in the above equation reproduces Eq. (54), at the leading order. On the other hand for  $\lambda = 0$ , we have  $\bar{m}_{\text{dyn}}^2 = 0$ . This shows from Eq. (53), that for pure cubic self interaction  $\langle \phi^2 \rangle \rightarrow \infty$  at late times. This is consistent with the rolling down and runaway disaster expected in a pure cubic potential. If we now ‘turn on’ a small  $\lambda$  value, we have from Eq. (55),

$$\bar{m}_{\text{dyn}}^2 = \frac{9\lambda}{16\pi^2} (1 + \mathcal{O}(\lambda/\bar{\beta}^2)) \quad (56)$$

The above result certainly is a manifestation of the fact that the quartic plus cubic self interaction potential is always bounded from below opposed to the pure cubic potential, no matter how small the quartic coupling is.

In order to find out a resummed expression for the quartic vertex function, we next *promote* the  $\langle \phi^2 \rangle$  appearing in Eq. (50) to *non-perturbative* level, so that  $\langle \phi^2 \rangle$  now stands for the bubble created by the exact propagator. The exact propagator can then be approximated into a daisy-like Feynman graph owing to the self interactions and considering only the local parts of associated loops and then again making them exact and so on, as depicted in Fig. 4. Using now Eq. (53) for the dynamical mass into Eq. (50), we simply obtain the resummed result

$$\frac{\lambda_{\text{eff,loc}}}{\lambda} = 1 - \frac{9\lambda}{32\pi^2 \bar{m}_{\text{dyn}}^2} + \frac{135\lambda^2}{1024\pi^4 \bar{m}_{\text{dyn}}^4} \quad (57)$$

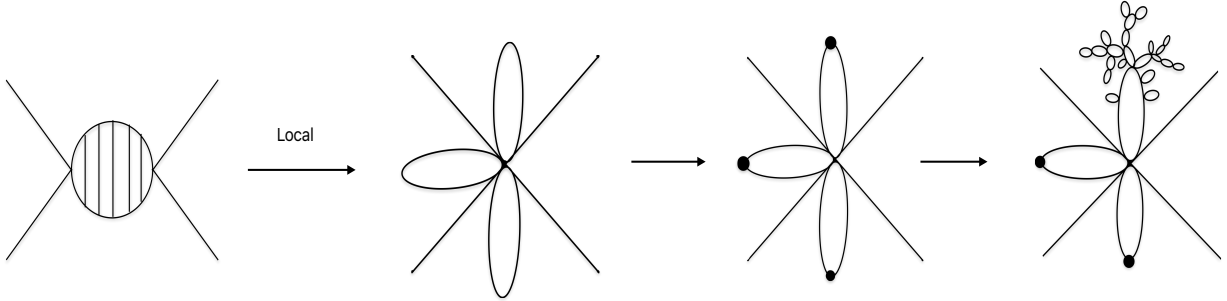


Figure 4: *The resummed quartic vertex function via the dynamical mass generation from purely local contributions. A dot over a propagator indicates that it is exact. These exact propagators are then essentially represented by daisy-like Feynman graphs. Similar argument holds for the resummed cubic vertex as well. See main text for discussion.*

Note that each of the terms appearing above, by the virtue of the appearance of the dynamical mass, is non-perturbative. Now for the quartic self interaction only, we have from Eq. (54)

$$\frac{\lambda_{\text{eff,loc}}}{\lambda} \Big|_{\bar{\beta} \rightarrow 0} = 1 - \frac{3\sqrt{3\lambda}}{8\pi} + \frac{45\lambda}{64\pi^2} + \mathcal{O}(\lambda^{3/2}) \quad (58)$$

Clearly, the above series is converging for  $\lambda < 1$ . Thus if we take for example,  $\lambda \sim 0.1$ , we have from Eq. (58)

$$\frac{\lambda_{\text{eff,loc}}}{\lambda} \Big|_{\bar{\beta} \rightarrow 0} \approx 1 - 0.058$$

indicating about 6% decrease in the value to the quartic coupling at late times. For any  $\lambda \lesssim \mathcal{O}(1)$ , there will be reduction in the quartic coupling. Such decrease essentially manifests strong quantum fluctuations.

On the other hand for  $\lambda \rightarrow 0$ , we have from Eq. (57), Eq. (56)

$$\frac{\lambda_{\text{eff,loc}}}{\lambda} \Big|_{\lambda \rightarrow 0} \approx 1 - 0.083, \quad (59)$$

showing around 8% decrease, irrespective of the value of any coupling, as dictated by Eq. (56). We have depicted the variation of  $\lambda_{\text{eff,loc}}/\lambda$ , Eq. (57), in Fig. 5 with respect to the tree level coupling parameters.

In order to find out the above resummed results, we used the dynamically generated mass at late times. We now wish to attempt below an interesting resummation technique inspired by the renormalisation group, proposed recently in [48, 49]. This formalism was applied recently in [51, 52], in order to compute the non-perturbative vacuum expectation values of the scalar field  $\phi$  as well the dynamically generated mass. We rewrite Eq. (33) as

$$\Delta\lambda = \frac{3\lambda\mathcal{N}}{2^4\pi^2} - \frac{15\lambda^2\mathcal{N}^2}{2^8\pi^4} \quad (60)$$

where  $\mathcal{N} = Ht$  is the number of de Sitter  $e$ -foldings and we have abbreviated

$$\Delta\lambda = - \left( \frac{\lambda_{\text{eff,loc}}(a)}{\lambda} - 1 \right)$$



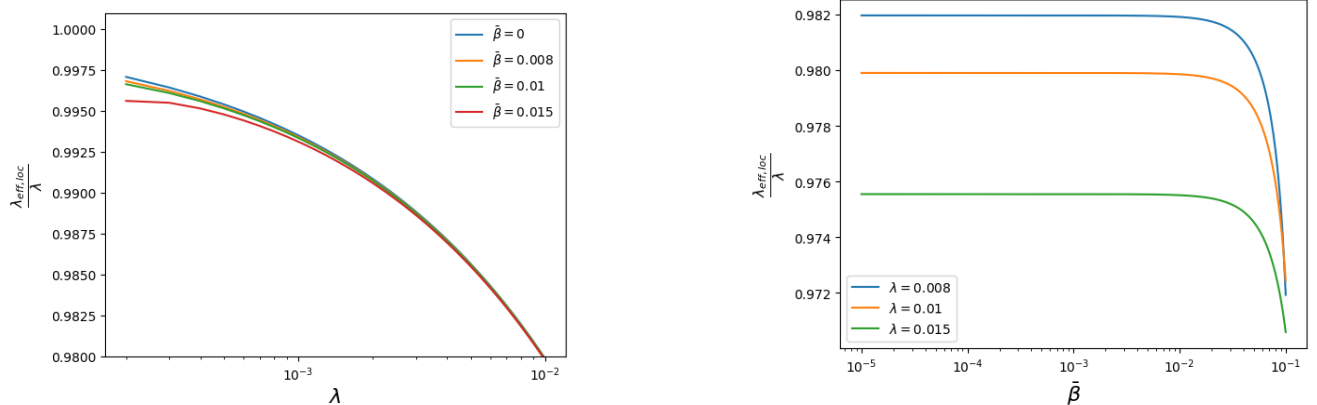


Figure 5: Variation of the resummed value of the quartic vertex function, Eq. (57), with respect to the tree level coupling parameters. See main text for discussion.

Following [48, 49], we differentiate Eq. (60) once with respect to  $\mathcal{N}$  to have the first order differential equation

$$\frac{\partial \Delta \lambda}{\partial \mathcal{N}} = \frac{3\lambda}{2^4 \pi^2} - \frac{15\lambda^2 \mathcal{N}}{2^7 \pi^4} \quad (61)$$

Using Eq. (60) we now replace the  $e$ -folding in the favour of  $\Delta \lambda$ , so that the equation is now promoted to non-perturbative level

$$\frac{\partial \Delta \lambda}{\partial \mathcal{N}} = -\frac{5\lambda}{2^3 \pi^2} \left( \Delta \lambda - \frac{3}{10} \right) \quad (62)$$

We integrate the above equation and find as  $\mathcal{N} \gg 1$ , we must have

$$\frac{\lambda_{\text{eff, loc}}}{\lambda} = 1 - 0.3 \quad (63)$$

which shows 30% decrease in the quartic coupling! This seems a little bit peculiar, in particular because the result holds irrespective of any value(s) of the coupling(s). Analogous result holds for the cubic vertex function, Eq. (48), as well. Owing to this, we are not sure whether Eq. (63) is a physically acceptable result. To the best of our understanding, it seems that the resummation proposal of [48, 49] will give satisfactory results if we attempt to deal with the expectation value of some operator, which satisfies some equation of motion, such as  $\langle \phi \rangle$  and  $\langle \phi^2 \rangle$ , as of [51, 52]. In other words, the same resummation procedure is likely to work well when we compute any correlation function of the scalar,  $\langle \phi^n \rangle$ . Thus for example for the present problem, instead of attempting a direct resummation of the vertex function from Eq. (33) as above, one should instead do the same for  $\langle \phi^2 \rangle$  in Eq. (50) while applying the aforementioned resummation technique.

Likewise for the cubic vertex function, Eq. (48), we obtain

$$\frac{\bar{\beta}_{\text{eff, loc}}}{\bar{\beta}} = 1 - \frac{9\lambda}{32\pi^2 \bar{m}_{\text{dyn}}^2} + \frac{27\lambda^2}{256\pi^4 \bar{m}_{\text{dyn}}^4} \quad (64)$$

showing both the effective quartic and cubic coupling strengths have similar behaviour with respect to the variation of the tree level coupling parameters,  $\lambda$  and  $\bar{\beta}$ , as depicted in Fig. 6.

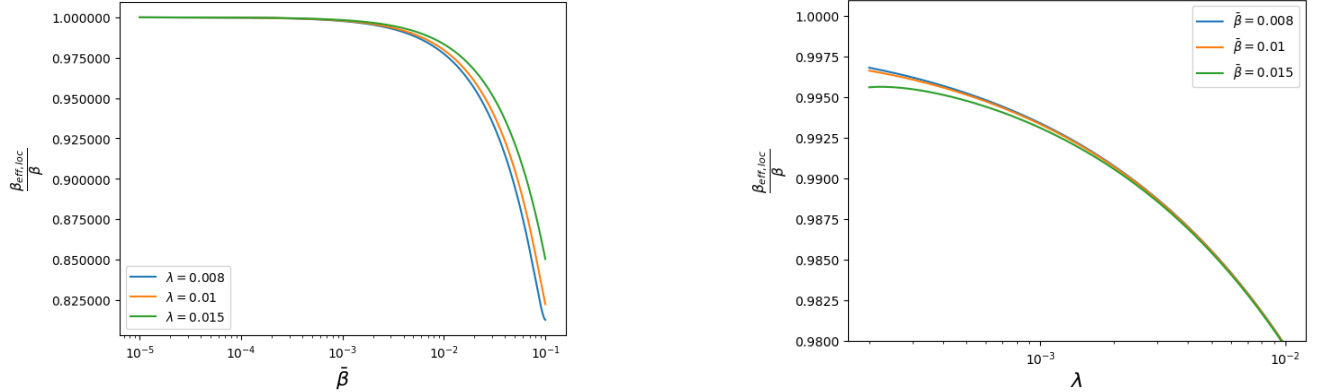


Figure 6: Variation of the resummed value of the cubic vertex function, Eq. (58), with respect to the tree level coupling parameters. See main text for discussion.

## 6 Discussion

In this paper we have considered the effect of the late time non-perturbative secular growth present in a self interacting, massless and minimally coupled quantum scalar field on the vertex functions in the inflationary de Sitter background. We have considered quartic and quartic plus cubic self interaction potentials in four spacetime dimensions, and have considered 4- and 3-point vertices. We have done explicit computations up to two loop for these vertex functions and have focused on the purely local part of them, in which case the vertices shrink to single points. The corresponding perturbative expressions for the vertex functions are given respectively by Eq. (33), Eq. (48). We have next assigned resummed values to the secular logarithms of these vertex functions in terms of the dynamically generated late time mass of the scalar field in Section 5. Since the dynamical mass essentially involves non-perturbative resummation of the local part of the self energy, the results we have obtained for the vertex functions are also non-perturbative, as we have argued in Section 5 (Eq. (57), Eq. (64)). As we have also mentioned in the main text of this paper, certainly this phenomenon can have no flat spacetime analogue.

We have seen that the secular effect and the dynamical mass generation reduces the resummed vertex functions compared to their tree level values, Fig. 5, Fig. 6. Such reduction in the effective vertex functions or couplings indicate changes in the value of the correlation function or the dynamical mass, such as Eq. (51), Eq. (54).

Now, what happens to the partly local and purely local vertex functions, appearing in, for example in Eq. (20)? At least for the partly local contributions (i.e., those with channel structure and without any integration), there are logarithms of the scale factor. Such logarithms appear from the Taylor expansion of a term like  $a^{d+\epsilon}/\epsilon$ . On the other hand, such term comes from the local part of the square of the Feynman propagator, Eq. (12). Thus it seems that we may replace these logarithms by the dynamical mass as well. Nevertheless, the full computation of any such vertex function which is not *purely* local must involve the in-in or the Schwinger-Keldysh formalism owing to the non-coincidence expressions for the propagator. In this case we will need all the four kind of propagators mentioned in Section 2 [68, 69, 70]. Apart from this, it seems also an interesting task to understand the results found in this paper from the perspective of a non-perturbative effective action. We wish to come back to this issue in a future work.

## A The diagrams with purely non-local contributions but no non-vanishing flat spacetime limit

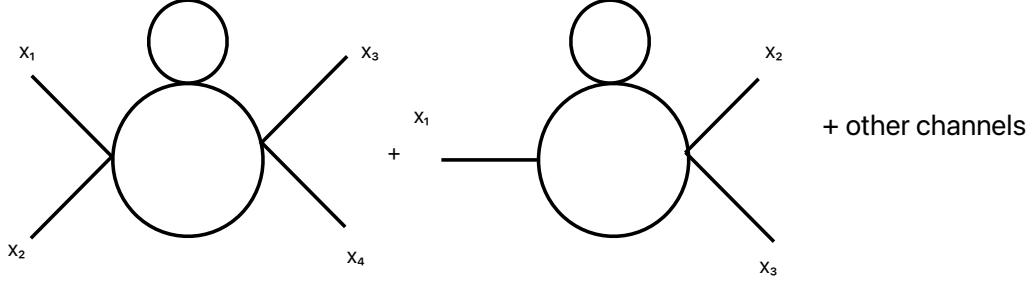


Figure 7: *Two loop diagrams which are vanishing after renormalisation in flat spacetime, but non-vanishing in de Sitter due to the secular logarithms. However, these diagrams do not yield any purely local contribution to the quartic or cubic vertex functions and hence do not affect the main results of this paper.*

In this appendix, we wish to discuss the diagrams, [Fig. 7](#), which do not yield any purely local contributions to the vertex functions, yet they yield some non-local contribution by the virtue of the secular logarithm. For the quartic vertex, the corresponding contribution at two loop reads

$$\begin{aligned}
-iV_+(x_1, x_2, x_3, x_4) &= \frac{i\lambda^3}{2^2} (a_1 a_2)^d \int d^d x a^d i\Delta(x, x) i\Delta_{++}(x_1, x) i\Delta_{++}(x, x_2) i\Delta_{++}(x_1, x_2) \delta^d(x_1 - x_3) \delta^d(x_2 - x_4) \\
&+ \frac{i\lambda^3}{2^2} (a_2 a_3)^d \int d^d x a^d i\Delta(x, x) i\Delta_{++}(x_2, x) i\Delta_{++}(x, x_3) i\Delta_{++}(x_2, x_3) \delta^d(x_1 - x_2) \delta^d(x_3 - x_4) \\
&+ \frac{i\lambda^3}{2^2} (a_3 a_1)^d \int d^d x a^d i\Delta(x, x) i\Delta_{++}(x_1, x) i\Delta_{++}(x, x_3) i\Delta_{++}(x_1, x_3) \delta^d(x_1 - x_4) \delta^d(x_2 - x_3)
\end{aligned} \tag{65}$$

We add to the above the one loop mass renormalisation counterterm (due to the quartic self interaction) diagram contribution

$$\begin{aligned}
-iV_+(x_1, x_2, x_3, x_4)|_{\text{CT}} &= \frac{i\lambda^2 \delta m_\lambda^2}{2} (a_1 a_2)^d \int d^d x a^d i\Delta_{++}(x_1, x) i\Delta_{++}(x, x_2) i\Delta_{++}(x_1, x_2) \delta^d(x_1 - x_3) \delta^d(x_2 - x_4) \\
&+ \frac{i\lambda^2 \delta m_\lambda^2}{2} (a_2 a_3)^d \int d^d x a^d i\Delta_{++}(x_2, x) i\Delta_{++}(x, x_3) i\Delta_{++}(x_2, x_3) \delta^d(x_1 - x_2) \delta^d(x_3 - x_4) \\
&+ \frac{i\lambda^2 \delta m_\lambda^2}{2} (a_3 a_1)^d \int d^d x a^d i\Delta_{++}(x_1, x) i\Delta_{++}(x, x_3) i\Delta_{++}(x_1, x_3) \delta^d(x_1 - x_4) \delta^d(x_2 - x_3)
\end{aligned} \tag{66}$$

Substituting now [Eq. \(10\)](#) for  $i\Delta(x, x)$  into [Eq. \(65\)](#), and [Eq. \(11\)](#) into [Eq. \(66\)](#) for  $\delta m_\lambda^2$ , we see that the the divergence

of Eq. (65) cancels, leaving us with an ultraviolet finite integral

$$\begin{aligned}
-iV_+(x_1, x_2, x_3, x_4)|_{2\text{loop, Ren.}}^{(4)} &= \frac{i\lambda^3 H^2}{2^4 \pi^2} (a_1 a_2)^d \int d^4 x a^4 \ln a i\Delta_{++}(x_1, x) i\Delta_{++}(x, x_2) i\Delta_{++}(x_1, x_2) \delta^d(x_1 - x_3) \delta^d(x_2 - x_4) \\
&+ \frac{i\lambda^3 H^2}{2^4 \pi^2} (a_2 a_3)^d \int d^4 x a^4 \ln a i\Delta_{++}(x_2, x) i\Delta_{++}(x, x_3) i\Delta_{++}(x_2, x_3) \delta^d(x_1 - x_2) \delta^d(x_3 - x_4) \\
&+ \frac{i\lambda^3 H^2}{2^4 \pi^2} (a_3 a_1)^d \int d^4 x a^4 \ln a i\Delta_{++}(x_1, x) i\Delta_{++}(x, x_3) i\Delta_{++}(x_1, x_3) \delta^d(x_1 - x_4) \delta^d(x_2 - x_3)
\end{aligned} \tag{67}$$

It is easy to see that the above integral does not yield any purely local contribution. Also, the above integral vanishes in the flat spacetime limit,  $a = 1$ .

Likewise for the cubic vertex, i.e. the second of Fig. 7, we have

$$\begin{aligned}
-iV_+(x_1, x_2, x_3)|_{2\text{loop}} &= \frac{i\beta\lambda^2}{2^2} (a_1 a_2)^d \int d^d x a^d i\Delta(x, x) i\Delta_{++}(x_1, x) i\Delta_{++}(x, x_2) i\Delta_{++}(x_1, x_2) \delta^d(x_2 - x_3) \\
&+ \frac{i\lambda^3}{2^2} (a_2 a_3)^d \int d^d x a^d i\Delta(x, x) i\Delta_{++}(x_2, x) i\Delta_{++}(x, x_3) i\Delta_{++}(x_2, x_3) \delta^d(x_1 - x_3) \\
&+ \frac{i\lambda^3}{2^2} (a_3 a_1)^d \int d^d x a^d i\Delta(x, x) i\Delta_{++}(x_1, x) i\Delta_{++}(x, x_3) i\Delta_{++}(x_1, x_3) \delta^d(x_1 - x_2)
\end{aligned} \tag{68}$$

which can be renormalised as of Eq. (65) to yield an integral which has only non-local contribution, via the secular logarithm. Both the above and Eq. (67) shows a qualitative difference of quantum field theory result of the de Sitter and the flat spacetime.

## References

- [1] S. Weinberg, *Cosmology*, Oxford Univ. Press (2009).
- [2] V. Mukhanov, *Physical Foundations of Cosmology*, Cambridge University Press, 2005.
- [3] N. C. Tsamis and R. P. Woodard, *Relaxing the cosmological constant*, Phys. Lett. B301, 351 (1993).
- [4] C. Ringeval, T. Suyama, T. Takahashi, M. Yamaguchi and S. Yokoyama, *Dark energy from primordial inflationary quantum fluctuations*, Phys. Rev. Lett.105, 121301 (2010) [arXiv:1006.0368 [astro-ph.CO]].
- [5] S. P. Miao, N. C. Tsamis and R. P. Woodard, *Summing inflationary logarithms in nonlinear sigma models*, JHEP **03**, 069 (2022) [arXiv:2110.08715 [gr-qc]].
- [6] N. Dadhich, *On the measure of spacetime and gravity*, Int. J. Mod. Phys. D20, 2739-2747 (2011) [arXiv:1105.3396 [gr-qc]].
- [7] T. Padmanabhan and H. Padmanabhan, *CosMIn: The Solution to the Cosmological Constant Problem*, Int. J. Mod. Phys. D22, 1342001 (2013) [arXiv:1302.3226 [astro-ph.CO]].
- [8] L. Alberte, P. Creminelli, A. Khmelnitsky, D. Pirtskhalava and E. Trincherini, *Relaxing the Cosmological Constant: a Proof of Concept*, JHEP12, 022 (2016) [arXiv:1608.05715 [hep-th]].

- [9] S. Appleby and E. V. Linder, *The Well-Tempered Cosmological Constant*, JCAP07, 034 (2018) [arXiv:1805.00470 [gr-qc]].
- [10] A. Khan and A. Taylor, *A minimal self-tuning model to solve the cosmological constant problem*, JCAP **10**, 075 (2022) [arXiv:2201.09016 [astro-ph.CO]].
- [11] O. Evnin and K. Nguyen, *Graceful exit for the cosmological constant damping scenario*, Phys. Rev. D **98**, no.12, 124031 (2018) doi:10.1103/PhysRevD.98.124031 [arXiv:1810.12336 [gr-qc]].
- [12] E. G. Floratos, J. Iliopoulos and T. N. Tomaras, *Tree Level Scattering Amplitudes in De Sitter Space diverge*, Phys. Lett. B197, 373 (1987).
- [13] N. A. Chernikov and E. A. Tagirov, *Quantum theory of scalar fields in de Sitter space-time*, Ann. Inst. H. Poincare Phys. Theor. A **9**, 109 (1968)
- [14] T. S. Bunch and P. C. W. Davies, *Quantum Field Theory in de Sitter Space: Renormalization by Point Splitting*, Proc. Roy. Soc. Lond. A **360**, 117-134 (1978).
- [15] A. D. Linde, *Scalar Field Fluctuations in Expanding Universe and the New Inflationary Universe Scenario*, Phys. Lett. B **116**, 335-339 (1982).
- [16] A. A. Starobinsky, *Dynamics of Phase Transition in the New Inflationary Universe Scenario and Generation of Perturbations*, Phys. Lett. B **117**, 175-178 (1982).
- [17] B. Allen, *Vacuum States in de Sitter Space*, Phys. Rev. D **32**, 3136 (1985).
- [18] B. Allen and A. Folacci, *Massless minimally coupled scalar field in de Sitter space*, Phys. Rev. D **35**, 3771 (1987).
- [19] G. Karakaya and V. K. Onemli, *Quantum effects of mass on scalar field correlations, power spectrum, and fluctuations during inflation*, Phys. Rev. D**97**, no.12, 123531 (2018) [arXiv:1710.06768 [gr-qc]].
- [20] V. K. Onemli and R. P. Woodard, *Superacceleration from massless, minimally coupled  $\phi^4$* , Class. Quant. Grav.**19**, 4607 (2002) [arXiv:gr-qc/0204065 [gr-qc]].
- [21] T. Brunier, V. K. Onemli and R. P. Woodard, *Two loop scalar self-mass during inflation*. Class. Quant. Grav. **22**, 59 (2005) [gr-qc/0408080].
- [22] E. O. Kahya, V. K. Onemli and R. P. Woodard, *A Completely Regular Quantum Stress Tensor with  $w < -1$* , Phys. Rev. D**81**, 023508 (2010) [arXiv:0904.4811 [gr-qc]].
- [23] D. Boyanovsky, *Condensates and quasiparticles in inflationary cosmology: mass generation and decay widths*, Phys. Rev. D**85**, 123525 (2012) [arXiv:1203.3903 [hep-ph]].
- [24] V. K. Onemli, *Vacuum Fluctuations of a Scalar Field during Inflation: Quantum versus Stochastic Analysis*, Phys. Rev. D**91**, 103537 (2015) [arXiv:1501.05852 [gr-qc]].
- [25] T. Prokopec and E. Puchwein, *Photon mass generation during inflation: de Sitter invariant case*, JCAP **0404**, 007 (2004) [astro-ph/0312274].
- [26] S. P. Miao and R. P. Woodard, *Leading log solution for inflationary Yukawa*, Phys. Rev. D **74**, 044019 (2006) [gr-qc/0602110].
- [27] T. Prokopec, N. C. Tsamis and R. P. Woodard, *Stochastic Inflationary Scalar Electrodynamics*, Annals Phys.**323**, 1324 (2008) [arXiv:0707.0847 [gr-qc]].

- [28] J. H. Liao, S. P. Miao and R. P. Woodard, *Cosmological Coleman-Weinberg Potentials and Inflation*, Phys. Rev. D**99**, no.10, 103522 (2019) [arXiv:1806.02533 [gr-qc]].
- [29] S. P. Miao, L. Tan and R. P. Woodard, *Bose-Fermi cancellation of cosmological Coleman-Weinberg potentials*, Class. Quant. Grav.**37**, no.16, 165007 (2020) [arXiv:2003.03752 [gr-qc]].
- [30] D. Glavan and G. Rigopoulos, *One-loop electromagnetic correlators of SQED in power-law inflation*, JCAP**02**, 021 (2021) [arXiv:1909.11741 [gr-qc]].
- [31] G. Karakaya and V. K. Onemli, *Quantum Fluctuations of a Self-interacting Inflaton*, arXiv:1912.07963.
- [32] J. A. Cabrer and D. Espriu, *Secular effects on inflation from one-loop quantum gravity*, Phys. Lett. B **663**, 361-366 (2008) [arXiv:0710.0855 [gr-qc]].
- [33] T. Prokopec and R. P. Woodard, *Production of massless fermions during inflation*, JHEP **10**, 059 (2003) [arXiv:astro-ph/0309593 [astro-ph]].
- [34] S. Boran, E. O. Kahya and S. Park, *Quantum gravity corrections to the conformally coupled scalar self-mass-squared on de Sitter background. II. Kinetic conformal cross terms*, Phys. Rev. D **96**, no.2, 025001 (2017) [arXiv:1704.05880 [gr-qc]].
- [35] G. Moreau and J. Serreau, *Backreaction of superhorizon scalar field fluctuations on a de Sitter geometry: A renormalization group perspective*, Phys. Rev. D**99**, no.2, 025011 (2019) [arXiv:1809.03969 [hep-th]].
- [36] G. Moreau and J. Serreau, *Stability of de Sitter spacetime against infrared quantum scalar field fluctuations*, Phys. Rev. Lett. **122**, no. 1, 011302 (2019) [arXiv:1808.00338 [hep-th]].
- [37] F. Gautier and J. Serreau, *Scalar field correlator in de Sitter space at next-to-leading order in a  $1/N$  expansion*, Phys. Rev. D**92**, no.10, 105035 (2015) [arXiv:1509.05546 [hep-th]].
- [38] J. Serreau, *Renormalization group flow and symmetry restoration in de Sitter space*, Phys. Lett. B**730**, 271 (2014) [arXiv:1306.3846 [hep-th]].
- [39] J. Serreau, *Nonperturbative infrared enhancement of nonGaussian correlators in de Sitter space*, Phys. Lett. B**728**, 380 (2014) [arXiv:1302.6365 [hep-th]].
- [40] J. Serreau and R. Parentani, *Nonperturbative resummation of de Sitter infrared logarithms in the large- $N$  limit*, Phys. Rev. D**87**, 085012 (2013) [arXiv:1302.3262 [hep-th]].
- [41] R. Z. Ferreira, M. Sandora and M. S. Sloth, *Patient Observers and Non-perturbative Infrared Dynamics in Inflation*, JCAP**02**, 055 (2018) [arXiv:1703.10162 [hep-th]].
- [42] S. Weinberg, *Quantum contributions to cosmological correlations*, Phys. Rev. D **72**, 043514 (2005).
- [43] C. P. Burgess, L. Leblond, R. Holman and S. Shandera, *Super-Hubble de Sitter Fluctuations and the Dynamical RG*, JCAP**03**, 033 (2010) [arXiv:0912.1608 [hep-th]].
- [44] C. P. Burgess, R. Holman and G. Tasinato, *Open EFTs, IR effects & late-time resummations: systematic corrections in stochastic inflation*, JHEP**01**, 153 (2016) [arXiv:1512.00169 [gr-qc]].
- [45] A. Youssef and D. Kreimer, *Resummation of infrared logarithms in de Sitter space via Dyson-Schwinger equations: the ladder-rainbow approximation*, Phys. Rev. D**89**, 124021 (2014) [arXiv:1301.3205 [gr-qc]].

- [46] M. Baumgart and R. Sundrum, *De Sitter Diagrammar and the Resummation of Time*, arXiv:1912.09502.
- [47] H. Kitamoto, *Infrared resummation for derivative interactions in de Sitter space*, Phys. Rev. D **100**, no.2, 025020 (2019) [arXiv:1811.01830 [hep-th]].
- [48] A. Y. Kamenshchik and T. Vardanyan, *Renormalization group inspired autonomous equations for secular effects in de Sitter space*, Phys. Rev. D **102**, no.6, 065010 (2020) [arXiv:2005.02504 [hep-th]].
- [49] A. Y. Kamenshchik, A. A. Starobinsky and T. Vardanyan, *Massive scalar field in de Sitter spacetime: a two-loop calculation and a comparison with the stochastic approach*, Eur. Phys. J. C **82**, no.4, 345 (2022).
- [50] N. C. Tsamis and R. P. Woodard, *Stochastic quantum gravitational inflation*, Nucl. Phys. B **724**, 295-328 (2005) [arXiv:gr-qc/0505115 [gr-qc]].
- [51] S. Bhattacharya, *Massless minimal quantum scalar field with an asymmetric self interaction in de Sitter spacetime*, JCAP **09**, 041 (2022) [arXiv:2202.01593 [hep-th]].
- [52] S. Bhattacharya and N. Joshi, *Non-perturbative analysis for a massless minimal quantum scalar with  $V(\phi) = \lambda\phi^4/4! + \beta\phi^3/3!$  in the inflationary de Sitter spacetime*, JCAP **03**, 058 (2023) [arXiv:2211.12027 [hep-th]].
- [53] S. Bhattacharya and M. D. Choudhury, *Non-perturbative  $\langle\phi\rangle$ ,  $\langle\phi^2\rangle$  and the dynamically generated scalar mass with Yukawa interaction in the inflationary de Sitter spacetime*, [arXiv:2308.11384 [hep-th]].
- [54] S. Bhattacharya, N. Joshi and K. Roy, *Resummation of local and non-local scalar self energies via the Schwinger-Dyson equation in de Sitter spacetime*, [arXiv:2310.19436 [hep-th]].
- [55] A. A. Starobinsky, *Stochastic de sitter (inflationary) stage in the early universe*, Lect. Notes Phys. **246**, 107-126 (1986).
- [56] A. A. Starobinsky and J. Yokoyama, *Equilibrium state of a selfinteracting scalar field in the De Sitter background*, Phys. Rev. D **50**, 6357-6368 (1994) [arXiv:astro-ph/9407016 [astro-ph]].
- [57] G. Cho, C. H. Kim and H. Kitamoto, *Stochastic Dynamics of Infrared Fluctuations in Accelerating Universe*, doi:10.1142/9789813203952\_0018 [arXiv:1508.07877 [hep-th]].
- [58] T. Prokopec, *Late time solution for interacting scalar in accelerating spaces*, JCAP **11**, 016 (2015) [arXiv:1508.07874 [gr-qc]].
- [59] B. Garbrecht, G. Rigopoulos and Y. Zhu, *Infrared correlations in de Sitter space: Field theoretic versus stochastic approach*, Phys. Rev. D **89**, 063506 (2014) [arXiv:1310.0367 [hep-th]].
- [60] V. Vennin and A. A. Starobinsky, *Correlation Functions in Stochastic Inflation*, Eur. Phys. J. C **75**, 413 (2015).
- [61] D. Cruces, *Review on Stochastic Approach to Inflation*, Universe **8**, no.6, 334 (2022) [arXiv:2203.13852 [gr-qc]].
- [62] F. Finelli, G. Marozzi, A. A. Starobinsky, G. P. Vacca and G. Venturi, *Generation of fluctuations during inflation: Comparison of stochastic and field-theoretic approaches*, Phys. Rev. D **79**, 044007 (2009) [arXiv:0808.1786 [hep-th]].
- [63] T. Markkanen, A. Rajantie, S. Stopyra and T. Tenkanen, *Scalar correlation functions in de Sitter space from the stochastic spectral expansion*, JCAP **08**, 001 (2019) [arXiv:1904.11917 [gr-qc]].
- [64] T. Markkanen and A. Rajantie, *Scalar correlation functions for a double-well potential in de Sitter space*, JCAP **03**, 049 (2020) [arXiv:2001.04494 [gr-qc]].

- [65] K. Enqvist, R. J. Hardwick, T. Tenkanen, V. Vennin and D. Wands, *A novel way to determine the scale of inflation*, JCAP **02**, 006 (2018) [arXiv:1711.07344 [astro-ph.CO]].
- [66] R. L. Davis, *On dynamical mass generation in de Sitter space*, Phys. Rev. D **45**, 2155 (1992).
- [67] M. Beneke and P. Moch, *On dynamical mass generation in Euclidean de Sitter space*, Phys. Rev. D **87**, 064018 (2013) [arXiv:1212.3058 [hep-th]].
- [68] E. Calzetta and B. L. Hu, *Closed Time-Path Functional Formalism in Curved Spacetime: Application to Cosmological Back-Reaction Problems*, Phys. Rev. D **35**, 495 (1987).
- [69] P. Adshead, E. Calzetta and B. L. Hu, *Nonequilibrium quantum fields: Closed-time-path effective action, Wigner function, and Boltzmann equation*, Phys. Rev. D **37**, 2878 (1988).
- [70] P. Adshead, R. Easther and E. A. Lim, *The ‘in-in’ Formalism and Cosmological Perturbations*, Phys. Rev. D **80**, 083521 (2009) [arXiv:0904.4207 [hep-th]].
- [71] M. E. Peskin and D. V. Schroeder, *An introduction to quantum field theory*, Addison-Wesley, USA (1995).